



# **High-Resolution Seismic Reflection/Refraction Imaging from Interstate 10 to Cherry Valley Boulevard, Cherry Valley, Riverside County, California: Implications for Water Resources and Earthquake Hazards**

**G. Gandhok<sup>1</sup>, R. D. Catchings<sup>1</sup>, M.R. Goldman<sup>1</sup>, E. Horta<sup>1</sup>, M. J. Rymer<sup>1</sup>, P. Martin<sup>2</sup>, and A. Christensen<sup>2</sup>**

Open-File Report 99-320

1999

This report is preliminary and has not been reviewed for conformity with U. S. Geological Survey editorial standards or with the North American Stratigraphic Code. Any use of product names is for descriptive purposes only and does not imply endorsement by the U. S. Government.

U. S. Geological Survey

<sup>1</sup>Menlo Park, California

<sup>2</sup>San Diego, California

## **Introduction**

This report is the second of two reports on seismic imaging investigations conducted by the U.S. Geological Survey (USGS) during the summers of 1997 and 1998 in the Cherry Valley area in California (Figure 1a). In the first report (Catchings et al., 1999), data and interpretations were presented for four seismic imaging profiles (CV-1, CV-2, CV-3, and CV-4) acquired during the summer of 1997. In this report, we present data and interpretations for three additional profiles (CV-5, CV-6, and CV-7) acquired during the summer of 1998 and the combined seismic images for all seven profiles. This report addresses both groundwater resources and earthquake hazards in the San Gorgonio Pass area because the shallow (upper few hundred meters) subsurface stratigraphy and structure affect both issues.

The cities of Cherry Valley and Beaumont are located approximately 130 km (~80 miles) east of Los Angeles, California along the southern alluvial fan of the San Bernardino Mountains (Figure 1b). These cities are two of several small cities that are located within San Gorgonio Pass, a lower-lying area between the San Bernardino and the San Jacinto Mountains. Cherry Valley and Beaumont are desert cities with summer daytime temperatures often well above 100° F. High water usage in the arid climate taxes the available groundwater supply in the region, increasing the need for efficient management of the groundwater resources. The USGS and the San Gorgonio Water District (SGWD) work cooperatively to evaluate the quantity and quality of groundwater supply in the San Gorgonio Pass region. To better manage the water supplies within the District during wet and dry periods, the SGWD sought to develop a groundwater recharge program, whereby, excess water would be stored in underground aquifers during wet periods (principally winter months) and retrieved during dry periods (principally summer months). The SGWD preferred a surface recharge approach because it could be less expensive than a recharging program based on injection wells. However, at an existing surface recharge site, surface recharge of the aquifer was limited by the presence of clay-rich layers that impede the downward percolation of the surface water. In boreholes, these clay-rich layers were found to extend from the near surface to about 50 m depth. If practical, the SGWD desired to relocate the recharge ponds to another location within the Cherry Valley-Beaumont area. This required that sites be found where the clay-rich layers were absent. The SGWD elected to explore for such sites by employing a combination of drilling and seismic techniques.

A number of near-surface faults have been suggested in the Cherry Valley-Beaumont area (Figure 1b). However, there may be additional unmapped faults that underlie the alluvial valley of San Gorgonio Pass. Because faults are known to act as barriers to lateral groundwater flow in alluvial groundwater systems, mapped and unmapped subsurface faults in the Cherry Valley-Beaumont area would likely influence groundwater flow and the lateral distribution of recharged water. These same faults may pose a significant hazard to the local desert communities and to greater areas of southern California due to the presence of lifelines (water, electrical, gas, transportation, etc.) that extend through San Gorgonio Pass to larger urban areas.

The three principal goals of the seismic investigation presented in this report were to laterally map the subsurface stratigraphic horizons, locate faults

that may act as barriers to groundwater flow, and measure velocities of shallow sediments that may give rise to amplified shaking during major earthquakes.

### **Local Geology and Tectonics**

The geology within the adjacent San Bernardino Mountains consists largely of pre-Cambrian metamorphic and igneous rocks (gneisses, schists, and Mesozoic granites; Jennings et al., 1977). Within San Gorgonio Pass, Pliocene sandstones, gravels, and clays are overlain by Quaternary alluvium (Jennings et al., 1977). Within the study area, Boyle Engineering Co. (1992) further categorized the upper 300 m of the Quaternary and Pliocene units as the San Timoteo Formation, the Old Red gravel, older alluvium, and recent alluvium. For purposes of discussion in the report, we will use the Boyle Engineering categorization for the shallow-depth lithology.

Along most of the seismic profiles, the upper 20 m of the Quaternary Alluvium unit consists of poorly sorted, unconsolidated gravel, sand, cobbles, and boulders. Underlying the Quaternary alluvium unit is the older alluvium unit, which consists of similar materials that are more consolidated. Beneath the older alluvium unit, the Old Red gravel unit consists of reddish-brown, poorly sorted, coarse gravel, sands, and is about 30 m thick in the Cherry Valley area. The San Timoteo Formation (~75 to 100 m below land surface) is the oldest geologic unit encountered in the boreholes at the existing recharge site, and it consists of poorly sorted to well-sorted, partly consolidated, fine-to-coarse sand, gravel and cobbles with thin clay layers (Boyle Engineering Co., 1992).

Tectonically, the Cherry Valley-Beaumont area is complex. The study area lies atop an alluvial fan that has been deposited on the southwest side of the San Bernardino Mountains. Major strands of the San Andreas fault trend through the San Bernardino Mountains and within the immediate study area. Strike-slip, thrust, and normal faults have been mapped in the vicinity of our seismic profiles (Figure 1b). Near the northern end of our seismic profiles, the Banning strand of the San Andreas fault has been mapped and consists of both thrust and strike-slip components that vary greatly in strike (Figure 1). Further south along the seismic profile, Matti et al. (1992) infer near-surface faults that are dominantly north-south-oriented and have normal components of motion. This tectonic complexity is caused largely by a change in the strike of the San Andreas fault system from a northwest orientation south of San Gorgonio Pass to one that is predominantly east-west within San Gorgonio Pass.

### **Seismic Survey**

#### **Data Acquisition**

In August 1998, the US Geological Survey acquired three high-resolution seismic reflection profiles along Noble Creek in Cherry Valley (Fig 1). These profiles are southward continuations of seismic reflection/refraction profiles acquired further north along Noble and Little San Gorgonio Creeks in July-August, 1997 (Catchings et al., 1999). The seismic profiles acquired in the present study (labeled CV-5, CV-6, and CV-7 in Figure 1a) range in length from about 715 m to about 1609 m (see Table 1). All three profiles had a northeast-southwest orientation.

Approximately 4 s of data were recorded using a linear array with as many as four Geometrics Strataview™ RX-60 seismographs, each with 60 active channels. The recorded data were stored on the hard drive of the Geometrics Strataview computers during field acquisition and later downloaded to 4-mm tape for permanent storage in SEG-Y format.

We used 40-Hz, single-element, Mark Products, L-40A™ geophones spaced at 5m intervals along the profiles. Seismic sources (shots), located at depths of about 0.5 m, were laterally spaced approximately every 5 m and were co-located (1m lateral offset) with the geophones along the profiles. The shots were generated by a BETSY Seisgun™ using 8-gauge shotgun blanks. Shot timing was determined electronically at the seismic source when the hammer electrically closed contact with the seisgun, sending an electrical signal to the seismograph.

Prior to acquiring the data, each recording site and shot point was measured with a meter tape and flagged to obtain the proper spacing. After the seismic data were acquired, we used differential Global Positioning System (GPS) measurements to locate recording sites and shot points with a theoretical accuracy of approximately 0.0001 m (see Appendices A, B, and C).

### Shot and Geophone Locations

Variations in shot and geophone locations and elevations can cause appreciable difficulty in stacking the reflection data and in accurately measuring the velocities if these variations are not known and considered in processing the seismic data. Large variations in the geometry of the shot and geophone arrays may also result in artifacts in the data that are interpreted as structure. Therefore, we present the line geometries (see Appendices A-C) for those who may wish to reprocess these data. To correlate variations in seismic velocities and seismic image anomalies with possible geometrical variations, we present graphical displays of the geometry along each profile, including shot point and geophone elevations, lateral variations from straight lines of shot point and geophone arrays, and fold. In many instances, abrupt changes in elevation can be correlated with apparent faults or major changes in stratigraphy on the seismic record, but apparent faults or stratigraphic changes that correlate with significant or abrupt changes in shot point and geophone geometry are likely to be artifacts of geometry. Areas with abrupt changes in fold may also contribute to the appearance of artifacts in the seismic data.

Table 1. Acquisition parameters for Cherry Valley seismic profiles. Distances are relative to the first shot point.

| Profile # | Orientation | Length of Geophone Profile (m) | Length of Shot Point Profile (m) | # of Shots | # of CDPs | Max Fold |
|-----------|-------------|--------------------------------|----------------------------------|------------|-----------|----------|
| CV-5      | NE-SW       | 715                            | 715                              | 143        | 286       | 143      |
| CV-6      | NE-SW       | 964                            | 964                              | 170        | 340       | 98       |
| CV-7      | NE-SW       | 1609                           | 1609                             | 317        | 646       | 119      |

## **Seismic Data Processing**

Both reflection and refraction data were available because we used a shoot-through configuration in acquiring the data. This type of data acquisition has numerous advantages over conventional data acquisition because detailed velocity data are available and folds are typically much greater. Detailed velocity data allow for better stacks in the shallow subsurface and also allow depths to be correctly calculated. The shoot-through acquisition method also allows for shallower imaging than is typically afforded in high-resolution seismology (Catchings et al., 1998).

### **Seismic Refraction Velocity Analysis**

We used two types of seismic data processing, refraction analysis and reflection processing. In refraction data processing, we used a seismic tomographic inversion method developed by Hole (1992), whereby, first arrivals on each seismic trace were used to measure detailed velocities for depths ranging from about 1 m below ground surface (bgs) to 250 m (~820 ft) bgs. For greater depths, velocities needed in seismic reflection stacking were determined using semblance and/or parabolic methods and apriori knowledge of the local geology. As described below, we used the velocities derived from these methods to convert the reflection time-images to depth-images and, where necessary, to migrate the seismic reflection images.

### **Seismic Reflection Processing**

Seismic reflection data processing was accomplished on a Sun Sparc 20<sup>TM</sup> computer using an interactive seismic processing package known as ProMax<sup>TM</sup>. The following steps were involved in data processing:

#### Geometry Installation

Lateral distances and elevations described above were used to define the geometrical set up of each profile. We installed the GPS-determined geometries (locations) into the ProMax<sup>TM</sup> processing package for each profile separately so that shot and receiver elevations and locations could be accounted for in the processing routine.

#### Trace Editing

Occasionally, bad coupling between the geophones and the ground, malfunctioning geophones, or cultural noises close to the seismic receivers resulted in unusually noisy traces at those locations. Traces representing those locations were edited. However, such traces were not always unsuitable for each shot gather; therefore, independent trace editing was employed for each shot gather.

#### Timing Corrections

Although the shotgun source electronically triggers the seismographs, there are small (~2 ms) delays between the electrical trigger and the actual shotgun explosions. We corrected for the delays by removing a constant 2 ms from the start time of each shot gather. At least two geophones (channels) were overlapped where individual seismograph systems joined. Any relative time variations among seismographs were removed by autocorrelating seismic traces at each overlap.

#### Elevation Statics

Elevation statics were also employed to correct for variations in elevations along the seismic profile. Velocities needed to make the corrections at each location were determined using the inversion methods described above.

#### Muting

To remove refractions and other arrivals that were not completely removed using filtering techniques, we used trace muting before and after stacking.

#### Bandpass Filtering

Most of the data of interest for seismic imaging and velocity measurement are well above 30 Hz, and most of the undesirable seismic data, such as surface waves and shear waves, were well below 30 Hz. Therefore, a bandpass filter with a low cut of 30 Hz was used to remove most surface and shear waves and cultural noise. Post-stack bandpasses were 10-20-200-400.

#### Gain Correction

An Automatic Gain Control value of 100 ms was added to the data.

#### F-K Filtering

Not all surface waves were removed by simple bandpass filtering. To remove surface waves and air waves that were not removed by bandpass filtering, we used F-K filtering, which filters on the basis of both frequency and velocity of the arrivals.

#### Velocity Inversion

As described above, velocities were measured from the seismic data using a computerized inversion routine.

#### Velocity Analysis

Velocities in the shallow section (~1 m to ~250 m; ~3 to 820 ft) were determined using velocity inversion techniques, but velocities in the deeper section were determined using semblance methods on CDP stacks.

#### Normal Moveout Correction

Channels that were progressively further from the seismic source experienced a progressively greater delay in the arrival of the seismic signal. To stack the seismic signal, this progressive delay was removed.

#### Stacking

To increase the strength of the seismic signal and to reduce the strength of random noises, we stacked the signal for each shot.

#### Depth Conversion

For stacked seismic reflection sections that were not migrated, we converted the time sections to depth sections using RMS velocities converted from the velocity analysis described above in the velocity section.

#### Migration

Due to the presence of numerous faults and diffraction points in the subsurface, diffraction hyperbolae were observed throughout the sections. We used pre-stack migration to collapse the diffraction hyperbolae to better identify the major faults and structures on depth sections.

## **Seismic Data**

### **Profile CV-5**

Profile CV-5 extended from Woodland Avenue to the intersection of Beaumont Avenue and Noble Creek (Fig. 1a). We used three RX-60 seismographs with 144 live channels to record approximately 143 shots along the

profile. Due to cultural features (gas lines, roads, etc.), one shot point was not utilized. Geophone elevations decreased by about 25 m from northeast to southwest (Fig. 2), and their locations varied from a straight line connecting the endpoints by less than 1 m over approximately 750 m of the array (Fig. 3). Similarly, most shot point elevations decreased by less than 25 m from northeast to southwest (Fig. 4), and their locations varied by less than 1 m from a straight-line array (Fig. 5). The minor variation in the linearity of the geophone and shot point arrays suggest that line geometry is unlikely to cause artifacts in the data that can be confused with structure.

Fold along the line varied linearly due to the stationary recording array. Maximum folds of approximately 143 were obtained near the center of the array but decreased to approximately 1 near the ends of the recording array (Fig. 6). This variation in fold suggests that the most reliable reflection image occurs near the center of the array. In practice, however, we've found that folds above about 30 are highly reliable for depths up to about 400 m (~1300 ft) in most areas in California. Thus, for the depths of interest to this investigation, we suggest that the seismic images are likely to be reliable across the entire profile.

### **Seismic Reflection Images Along Profile CV-5**

Stacked and migrated seismic reflection images to depths of approximately 200 m (~650 ft) along profile CV-5 are shown in figure 7. These data show numerous reflections from the near surface to a depth of 200 m bgs. Clear primary reflections are evident in the upper 120 to 160 m, below which, there may be reverberations. Test Well 1 was located within 10 m of the profile CV-5, thereby allowing principal reflections to be correlated with major lithologic units identified in the borehole (Fig. 7). The upper ~60 m correlate with the alluvial layers described by Boyle Engineering (1992), and they appear to be laterally continuous across the profile. Reflections corresponding to the Old Red gravel extend from about 60 m bgs to about 100 m bgs. Below about 100 m, the seismic signal becomes more reverberative within the San Timoteo Formation, as is frequently observed at the transition between sediments to harder rock.

The cumulative sedimentary section shows consistent vertical offsets of layers at several locations along the seismic profile, suggesting that the layers are faulted. Offsets at about meters 500 to 550, meters 350 to 400, and 200 to 250 are observed from the near-surface to depths of about 100 m.

### **Velocity Section Along Profile CV-5**

Seismic velocities along profile CV-5 range from about 400 m/s near the surface to about 2200 m/s at depths of about 200 m (~650 ft) (Fig. 8). Velocities ranging from about 400 m/s to about 1300 m/s correlate with the alluvial layers, and those from about 1400 m/s to about 2100 m/s correlate with the Old Red gravel. Velocities above 2100 m/s correlate with the San Timoteo Formation. The velocity data suggest a thickening of the alluvial units from the northeast to the southwest by nearly 100 percent along profile CV-5. The greatest thickening occurs southwest of meter 500, where a near-vertical velocity anomaly suggests a probable fault.

In unconsolidated alluvial environments, velocities of about 1500 m/s and higher correlate with saturated sediments (Schon, 1996), and velocities below

about 1500 m/s correlate with unsaturated sediments. This correlation between velocity and saturated sediments can be used to infer the water table if the water table is thick enough to propagate seismic waves. On the velocity section (Fig. 8), the 1500 m/s contour (shown in blue) suggests that a water table (perched or otherwise) is located within the upper part of the Old Red gravel.

### **Combined Velocity and Reflection Images**

The seismic velocity inversion model has been superimposed on the seismic reflection images for profile CV-5 (Fig. 9). Seismic reflection images are available for greater depths, but the combined velocity and reflection images show that velocity contours can be correlated with laterally continuous reflections and stratigraphic units identified from borehole logs. This combined image also aids in identifying lateral variations in stratigraphic units because the more consolidated units generally have higher velocities.

### **Profile CV-6**

Profile CV-6 originated near the intersection of Beaumont Avenue and Noble Creek and extended about 900 m southwestward (Fig. 1). We used three RX-60 seismographs with 180 live channels to record approximately 170 shots along the profile. Due to cultural features (gas lines, roads, etc.), 24 shot points were not utilized. Although data were recorded beneath the bridge at Beaumont Avenue, several consecutive shot points were not utilized because of the presence of a concrete liner within Noble Creek.

Geophone elevations decreased by about 30 m from northeast to southwest (Fig. 10), and their locations varied from a straight line connecting the endpoints by less than 5 m over approximately 964 m of the array (Fig. 11). Similarly, shot point elevations also decreased by about 30 m from northeast to southwest (Fig. 12), and their locations varied from a straight-line array by less than 6 m (Fig. 13). The minor variation in linearity of the geophone and shot-point arrays suggest that the line geometry is unlikely to cause artifacts in the data that can be confused with structure. Fold along the profile varied linearly due to the stationary recording array. Maximum folds of approximately 98 were obtained near the center of the array but decreased to approximately one near the ends of the recording array (Fig. 14), suggesting that the best-resolved images are near the center of the array.

### **Seismic Reflection Images along profile CV-6**

Stacked and migrated seismic reflection images to depths of approximately 200 m (~650 ft) along profile CV-6 are shown in figure 15. The northeasternmost end of profile CV-6 overlapped the southwesternmost end of CV-5 by approximately 10 m. These data also show numerous reflections from the near surface to 200 m, with clear primary reflections in the upper 120 to 140 m along most of the profile. However, more coherent and deeper reflections are apparent near the southwestern end of the profile.

### **Velocity Section along Profile CV-6**

The southwestern part of the profile CV-6 overlaps the northeastern part of CV-7 and extends 55 m southwest of the intersection of the two lines. Seismic velocities along profile CV-6 range from about 300 m/s near the surface to about

2400 m/s at depths of about 200 m (~650 ft) (Fig. 16). Velocities ranging from about 400 m/s to about 1300 m/s correlate with the alluvial layers, and those from about 1400 m/s to about 2000 m/s correlate with the Old Red gravel. Velocities above 2000 m/s correlate with the San Timoteo Formation. Unlike profile CV-5, the velocity data do not indicate much southwest thickening of the alluvial units along profile CV-6, which appear to be about 150 m thick. Velocity anomalies between meters 500 and 800 suggest vertical displacement of all units from the San Timoteo to the near-surface alluvial units.

The 1500 m/s velocity contour (blue), which we believe to correlate with the water table, also shows lateral offset near meters 500 and 800. Such a lateral variation in the depth to water table would be expected if the apparent faults

inhibit lateral groundwater flow. However, along the southwestern 600 m of the profile, there appears to be little southwestward dip associated with the 1500 m contour.

### **Combined Velocity and Reflection Images along profile CV-6**

The seismic velocity inversion model has been superimposed on the seismic reflection image for profile CV-6 (Fig. 17). The combined image shows the difference in reflection character between the alluvial (blue and green) strata and the more consolidated (yellow and red) strata. In general, the alluvial strata appears to be more laterally continuous.

Wells were not located along profile CV-6, but stratigraphic units can be correlated with those from profiles CV-5 and CV-7, both of which are located near wells with lithologic descriptions (Fig. 17). The upper ~100 m correlate with the alluvial layers, which appear to be largely sub-horizontal (with a slight southwestward dip) and are continuous along profile CV-6. Reflections corresponding to the Old Red gravel extend from about 100 m to about 150 m bgs. Reflections corresponding to the San Timoteo Formation are evident from about 150 to 200 m bgs and appear to be thicker and more coherent. The cumulative sedimentary section shows consistent vertical offsets of layers at several locations along the seismic profile, suggesting that the layers are faulted. Offsets at about meters 850, 725, and 575 respectively, are evident from the near surface to the bottom of the section.

### **Profile CV-7**

Profile CV-7 extended 30 m beyond (overlapped) the southwestern end of profile CV-6. The profiles were processed as two separate profiles because a distinct bend in Noble Creek resulted in appreciably different orientations of the two profiles. Profile CV-7 extended from its intersection with profile CV-6 to a second bend in Noble Creek near the I-10 freeway, a distance of approximately 1600 m. We used three RX-60 seismographs with 180 live channels to record approximately 317 shots along the profile. Due to cultural features (gas lines, roads, etc.), six shot points were not utilized. Geophone elevations decreased by about 37 m from northeast to southwest (Fig. 18), and their locations varied from a straight line connecting the endpoints by less than 7 m over approximately 1609 m of the array (Fig. 19). Similarly, most shot point elevations varied by less than 37 m from northeast to southwest (Fig. 20), and their locations varied by less

than 6 m from a straight-line array (Fig. 21). The minor variation in linearity of the geophone and shot point arrays suggest that line geometry is unlikely to cause artifacts in the data that can be confused with structure. Fold along the profile varied linearly due to the stationary recording array (Fig. 22). Maximum folds of approximately 119 were obtained near the center of the array but decreased to approximately one near the ends of the recording array. This variation in fold suggests that the reflection images are most reliable near the center of the profile.

### **Seismic Reflection Images along profile CV-7**

Stacked and migrated seismic reflection images to depths of approximately 250 m (~820 ft) along profile CV-7 are shown in figure 23. These data show numerous reflections from the near surface to the bottom of the section, with clear primary reflections in the upper ~150 m. The reflection section appears reverberative in the bottom 100 m, but we are not sure whether they are primary reflections or multiples. Because the reflections are not evenly spaced either laterally or vertically, we suggest that most of the reflections are probably not reverberations.

A borehole, with lithologic logs, was located about 100 m west of meter 600 of the profile CV-7. Information from this borehole permits a rough correlation between known stratigraphy and the seismic image. The seismic reflection image shows that the alluvium units are thickest in the northwestern part of the profile, where they are over 100 m thick. These alluvium layers gradually thin to the southwest, where they are about 75 m thick near the end of the profile. On the basis of the reflection data alone, it is not possible to determine the thickness of the Old Red gravel and the San Timoteo Formation, but the reflection data indicate that these more consolidated units do not have appreciable dip to the southwest along profile CV-7. The seismic reflection images show evidence of vertical-offset faulting along most of the profile.

### **Velocity Section along Profile CV-7**

Seismic velocities along profile CV-7 range from about 300 m/s near the surface to about 5000 m/s along an apparent horst structure near meter 600 of the seismic profile (Fig. 24). Along most of the profile, however, maximum velocities were slightly in excess of 4000 m/s at depths of about 250 m (820 ft). Velocities ranging from about 300 m/s to about 1300 m/s correlate with the alluvial layers, and those from about 1400 m/s to 2000 m/s correlate with the Old Red gravel. Velocities ranging from 2000 m/s to 3000 m/s probably correlate with the San Timoteo Formation, but velocities of about 4000 m/s and greater likely correspond to crystalline rocks.

The velocity data suggest thinning of the alluvial units from the northeast to the southwest by nearly 25% along profile CV-7. The thinning appears to be gradual, whereby, less alluvium was deposited on top of the underlying sedimentary and crystalline rocks. A series of horsts and graben are suggested by velocity contours that abruptly rise and fall along the section. These variations in the velocity contours extend to the near surface, suggesting that faults associated with basement horsts and graben extend to the near surface. Maximum vertical relief on the apparent horst and graben structures ranges from about 25 to 50 m.

The 1500 m/s contour (shown in blue) is consistent with the depth of the water table that was measured in the nearby well to the west. The 1500 m/s contour, which we suggest correlates with the water table, rises and falls by about 10 to 20 m over the horst and graben structures, suggesting that the faults associated with these structures act as barriers to lateral flow of groundwater.

#### **Combined Velocity and Reflection Images along profile CV-7**

The same general correlation between velocity and reflective character as found along the other two profiles is evident along profile CV-7. However, the combined seismic velocity and reflection image along CV-7 gives a more continuous and clearer image to greater depths (Fig. 25). In general, the alluvial layers have velocities less than 1300 m/s, the Old Red gravel varies in velocity between 1300m/s and 2000 m/s, and the San Timoteo Formation has velocities between 2000m/s and 3000 m/s. The reflection data and the velocity data suggest that these layers vary appreciably and consistently in depth. The vertical variation in depth of the alluvial layers above the horst and graben structures suggest that these faults were active during deposition of the alluvial layers.

### **Interpretation**

#### **Combined Profiles**

Structural variation in the upper few hundred meters between Woodland Avenue and the I-10 freeway are most apparent when viewing a composite image of all seismic profiles (Fig. 26 and Fig. 27). The composite data show that the deeper units, principally the Old Red gravel and the San Timoteo Formation have steep dips along profile CV-5. The San Timoteo Fm, in particular, appears to be vertically offset by as much as 100 m along profile CV-5, with the downthrown side on the southwest. The offset represents the largest vertical offset in strata observed along any of the seven profiles acquired in the Cherry Valley–Beaumont area. Both the reflections and the velocity contours representing the San Timoteo Formation dip sharply to the southwest, whereas, the reflections and the velocity contours representing the Quaternary alluvium dip only moderately. The gradient in surface topography as well as the Quaternary alluvium layers is greatest along profile CV-5. These alluvial layers extend into profile CV-6 and are consistent with the dip of the deeper layers. The near-surface alluvial layers thicken by nearly 100 percent along profile CV-5, with a maximum thickness of nearly 150 m. Southwest of this area of apparent faulting, the Old Red gravel and San Timoteo Formation are nearly horizontal except where they are locally faulted.

### **Summary and Conclusions**

The towns of Cherry Valley and Beaumont are located on alluvial fans of the southwestern San Bernardino Mountains. The stratigraphic sequences deposited here are somewhat typical of those deposited along alluvial fans, largely consisting of sand, gravel, clay, and boulders. In the Cherry Valley area, the upper 50 m consist of clay-rich deposits that likely extend along all the profiles (CV-1 through CV-7) from the existing surface recharge ponds in Cherry Valley to near the I-10 freeway. Along the northeasternmost seismic profiles (CV-1 and CV-3), the clay-rich Quaternary Alluvium deposits are only about 50 m thick but appear to thicken at several locations along apparent faults.

Northeast of Woodland Avenue, these layers appear to be no thicker than about 75 m, but southwest of Woodland Avenue, the clay-rich layers rapidly increase to a maximum thickness of about 150 m along a major fault structure. The Quaternary alluvial layers thin from about 150 m at Brookside Ave to about 80 m near the southwestern end of profile CV-7. Although we do not know if these clay-rich layers exist in northwest or southeast of the seismic profiles, deposits in the Noble Creek and Little San Gorgonio Creek drainage basins are probably not significantly different from the rest of the alluvial fan deposits. Thus, it is likely that surface recharge of the groundwater aquifer will be difficult at most locations in the Cherry Valley–Beaumont area.

Seismic velocities in water-saturated alluvial deposits are known to have seismic P-wave velocities of about 1500 m/s (Schon, 1996). The detailed velocity images from this study can therefore be used to infer lateral variations in the water table (perched and/or static) when the water table is thick enough to transmit seismic waves. Wells located along profile CV-3 and near profile CV-7 show that the 1500 m/s contour correlates with the water table observed in those wells. The correlation between velocity and the water level in Test Well 1, located near the northeastern end of CV-5, is inconclusive because: (1) The well is located several tens of meters off the seismic profile. (2) The water level identified in the well may be the deeper static water level, not a perched water level that would be first sensed by the seismic data. (3) Velocity information near the northeastern end of the profile, at the depth of the water table, is not available. (4) The northward continuation of the seismic section to the well location was not imaged, and fault complexity in that area probably affects the depth of the water table. Most of the wells, however, show a strong correlation between the 1500 m/s contour and the water level. Using the 1500 m/s contour as a guide to the water table, the velocity data suggest that the water table is closely aligned with the top of the Old Red gravel.

Because of the complex tectonics associated with the San Andreas fault in the San Gorgonio Pass area, it is not surprising that numerous smaller faults are imaged beneath the Quaternary alluvial cover in San Gorgonio Pass. In fact, some of these faults have been inferred by surface geologic mapping (Matti et al., 1992) (Fig. 28). Most of the smaller individual faults have apparent vertical offsets of about 10 m or less, but some appear to be a series of intense faults with cumulative vertical offsets of several tens of meters. Although these faults appear to be smaller faults, many are predominantly strike-slip faults, and because the seismic images only show the apparent vertical offset, the true vertical or horizontal offset is not known.

In addition to the smaller faults, there appear to be two areas (the northern end of profile CV-3 and the northern end of profile CV-5) with apparent vertical offsets between 50 m and 100 m and several areas with apparent vertical offsets of several tens of meters. These larger-offset faults probably represent significant faults that extend for appreciable distances through San Gorgonio Pass. The larger offset faults appear to correlate with significant bends in the drainages along the alluvial fan, suggesting that strike-slip motion has displaced the drainage laterally. Other similar bends can be seen in drainages further to the northwest and southeast, suggesting that the imaged faults have a northwesterly trend. Along profiles CV-6 and CV-7, a series of horsts and graben, with vertical offsets of several tens of meters are apparent in the seismic images. Similar fault

structures have been mapped at the surface by Matti et al. (1992), who refer to these faults as the “Beaumont Plain fault zone.” Matti et al. (1992) show these to be a series of NW-SE-oriented, en-echelon faults that are downthrown to the north and traverse late Quaternary alluvial deposits in the vicinity of Beaumont. However, our data show that these structures are more like horst and graben.

Most hazard assessments for the southern California area assume that most of the slip on the San Andreas fault zone occurs on the mapped traces of the fault. However, the number of imaged faults beneath the alluvial deposits of San Gorgonio Pass and their apparent vertical displacements suggest that an appreciable amount of the slip along the San Andreas fault zone at the latitude of San Gorgonio Pass is accommodated by these buried faults. Assessments that account for the slip on faults not visible at the surface would better estimate the overall slip rate and better assess strain accumulation and recurrence intervals.

Hazards related to strong ground motions in the San Gorgonio Pass area should be re-assessed. Lifelines that extend through San Gorgonio Pass to highly populated areas of southern California, including the Los Angeles metropolitan area may be affected by earthquakes on faults beneath San Gorgonio Pass or by regional earthquakes on other faults of the San Andreas fault zone. Low-velocity, unconsolidated sediments are known to amplify seismic waves and result in violent shaking (Borcherdt et al, 1975; Borcherdt and Glassmoyer, 1994). In the Cherry Valley–Beaumont area, low-velocity ( $V_p = 300$  m/s to 1200 m/s), unconsolidated units are as thick as 150 m. Critical lifelines, including the California Aqueduct, electrical power lines, gas lines, and transportation lines (cars, trains), would likely be impacted by large magnitude earthquakes on either the San Andreas or the faults imaged beneath San Gorgonio Pass.

#### **Data Availability**

Digital data from this report are available in SEG-Y format (with elevation and timing corrections applied) from R. D. Catchings at the address on the front of this report.

#### **Acknowledgements**

We thank Jeff Dingler, Andy Gallardo, Joseph Grow, Jose Rodriguez, and Scott Strohmeier for assistance in acquiring the seismic data. The project was funded by the San Gorgonio Pass Water Agency, and we particularly thank Steve Stockton for his assistance. Data acquisition and analysis was accomplished through cooperative efforts by the U.S. Geological Survey’s Geologic and Water Resources Divisions and the San Gorgonio Pass Water Agency.

#### **References**

Borcherdt, R. D., J. F. Gibbs, and K. R. Lajoie, 1975, Prediction of maximum earthquake intensity in the San Francisco Bay region, California, for large earthquakes on the San Andreas and Hayward faults, U.S. Geol. Surv. Misc. Field Studies Map MF-709, 11 pp., scale 1:125,000.

Borcherdt, R. D. and G. Glassmoyer, 1994, Influences of local geology on strong and weak ground motions recorded in the San Francisco Bay region and their implications for site-specific building code provisions, in the Loma Prieta,

California Earthquake of October 17, 1989 - Strong Ground Motion, U.S. Geol. Surv. Profess. Pap. 15512-A, 77-109.

Catchings, R. D., E. Horta, M.R. Goldman, M.J. Rymer, and T.R. Burdette, 1998a, High-resolution seismic imaging for environmental and earthquake hazards assessment at the Raychem Site, Menlo Park, California, U.S. Geol. Surv. Open-File Report 98-146, 37 pp.

Catchings, R. D., M. R. Goldman, W. H. K. Lee, M. J. Rymer and D. J. Ponti, 1998b, Faulting Apparently Related to the 1994 Northridge, California, earthquake and possible co-seismic origin of surface cracks in Potrero Canyon, Los Angeles County, California, Bull. Seis. Soc. America, 88, 1379-1391.

Catchings, R.D., G. Gandhok, M.R. Goldman, E. Horta, and M.J. Rymer, P. Martin, A. Christensen, 1999, High resolution seismic reflection/refraction imaging beneath Cherry Valley, Riverside County, California: Implications for water resources and earthquake hazards, U.S. Geol. Surv. Open-File Report 99-26, 58 pp.

Catchings, R.D. and W.H.K. Lee, 1996, Shallow velocity structure and Poisson's ratio at the Tarzana, California strong motion accelerometer site, Bull. Seis. Soc. America, 86, 1704-1713.

Hauksson, E., L. M. Jones, and K. Hutton, 1995, The 1994 Northridge earthquake sequence in California: Seismological and tectonic aspects, J. Geophys. Res., 97, 12,335-12,355.

Hole, J.A, 1992, Nonlinear high-resolution three-dimensional seismic travel time tomography, J. Geophys. Res., v. 97, p. 6553-6562.

Jennings, C.W., R.G. Strand, and T.H. Rogers, 1977, Geologic Map of California: California Geologic Data Map Series, Map No. 2, map scale 1:750,000.

Matti, J.C., D.M. Morton, and B.F. Cox, 1992, The San Andreas fault system in the vicinity of the central Transverse ranges province, southern California, U.S. Geol. Surv. Open-File Report 92-354.

Schon, J. H., 1996, Physical Properties of Rocks: Fundamentals and Principles of Petrophysics, Handbook of Geophysical Exploration, Seismic Exploration vol. 18, Elsevier Science, Inc., Tarrytown, New York.

### **List of Figures**

Figure 1a. Map of Cherry Valley showing location of seismic lines 5 through 7 (thick red lines) and 1 through 4 (thick gray lines).

Figure. 1b. Fault map of the San Gorgonio Pass Area, Southern California (from Matti et al., 1992) with seismic profiles (red lines) of the Cherry Valley area and other seismic profiles recently acquired by the USGS in the San Gorgonio Pass area.

Fig.2. Geophone elevation along CV-5. Elevation is relative to the topographically lowest shot point.

Figure.3. Geophone variation from a straight line connecting the first and last geophone along profile CV-5

Figure. 4. Variation in shot-point elevation along profile CV-5. Elevation is relative to the topographically lowest shot point along the profile.

Figure. 5. Variation in shot-point locations relative to a straight line connecting the end points along profile CV-5.

Figure. 6 Fold as function of CDP along CV-5.

18

Figure. 7. Stacked and migrated seismic reflection image along profile CV-5. Depth is relative to the topographically lowest shot point along the profile. Test Well 1 is shown in it's approximate geographic location with stratigraphic units described by Boyle Engineering (1992).

Figure. 8. Velocity inversion model along CV-5. Depth is relative to the topographically lowest shot point along the seismic profile.

Figure. 9. Stacked and migrated seismic reflection image along profile CV-5 with the velocity inversion model superimposed. The lithologic log from test well 1 is shown where it occurs geographically along the profile. The light blue contour below about 100 m is the 1500 m/s contour, which may coincide with a perched water table.

Figure.10. Variation in Geophone elevation along Profile CV-6 Elevation is relative to the topographically lowest shot point along the profile

Figure.11. Geophone variation from a straight line connecting the first and last geophone along profile CV-6

Figure. 12. Variation in shot point elevation along Line 6. Elevation is relative to the topographically lowest geophone along profile CV-6.

Figure.13. Shot point variation from a straight line connecting the first and last geophone along profile CV-6.

Figure. 14. Fold as a function of common depth point (cdp) along profile CV-6.

Figure. 15. Stacked and migrated seismic reflection image along profile CV-6. Depth is relative to the topographically lowest geophone along the profile.

Figure. 16. Seismic velocity inversion model along profile CV-6. Depth is relative to the topographically lowest geophone along the profile.

Figure. 17. Stacked and migrated seismic reflection image of the profile CV-6 with the velocity inversion model superimposed. Depth is relative to the topographically lowest shot point along the profile. The 1500 m/s contour (blue) may correlate with the water table.

Figure.18. Geophone elevation along profile CV-7. Elevation is relative to the topographically lowest geophone along the profile.

Figure.19. Geophone variation from a straight line connecting the first and last geophone in profile CV-7.

Figure.20. Variation in Shot point elevation along Profile CV-7. Elevation is relative to the topographically lowest shot point along the line.

Figure.21. Shot point variation from a straight line connecting the first and last shot point along Profile CV-7.

Figure. 22. Fold as a function of common depth point (cdp) along profile CV-7

Figure. 23. Stacked and migrated seismic reflection image along profile CV-7. Depth is relative to the topographically lowest geophone along the profile.

Figure. 24. Seismic velocity inversion model along profile CV-7. Depth is relative to the topographically lowest geophone along profile CV-7.

Figure. 25. Stacked and migrated seismic reflection image along profile CV-7 with velocity inversion model superimposed. Depth is relative to the topographically lowest shot point along the profile. The 1500 m/s contour (blue) apparently correlates with the water table.

Figure. 26a. Composite reflection-velocity images of the profiles CV-1, CV-2, CV-5, CV-6, and CV-7. Alluvial layers are highlighted with yellow. Test Well 1 is shown in its approximate geographical location along the profiles. The stratigraphy of the well is as follows: Yellow = alluvial layers, Red = Old Red gravel, and Green = San Timoteo Fm.

Figure. 26b. Composite reflection-velocity images of profiles CV-3, CV-4, CV-5, CV-6, and CV-7. Alluvial layers are highlighted with yellow. Test Well 1

is shown in its approximate geographical location along the profiles. The stratigraphy of the well is as follows: Yellow = alluvial layers, Red = Old Red gravel, and Green = San Timoteo Fm.

Figure. 27a Composite seismic velocity inversion models along profiles CV-1, CV-2, CV-5, CV-6, and CV-7 with the locations of wells near the seismic profiles. The 1500 m/s contour is show in blue and correlates with the water table in most wells. Faults are inferred by abrupt vertical changes in the velocity contours.

Figure. 27b. Composite seismic velocity inversion models along profiles CV-3, CV-4, CV-5, CV-6, and CV-7 with the locations of wells near the seismic profiles. The 1500 m/s contour is show in blue and correlates with the water table in most wells. Faults are inferred by abrupt vertical changes in the velocity contours.

Figure 28. Map of Cherry Valley showing location of seismic lines 1 through 7 (blue lines) with faults (red) mapped by Matti et al. (1992). The dashed green line is an inferred fault.

**Appendix A**  
**Cherry Valley Line 5**

| FFID | SP# | SP Dist. | SP Elev. | Geo# | Geo. Dist | Geo. Elev. |
|------|-----|----------|----------|------|-----------|------------|
| 1001 | 1   | 0        | 0        | 1    | 0         | 0          |
| 1002 | 2   | 5.1      | 0.1      | 2    | 5.19      | 0.15       |
| 1003 | 3   | 9.97     | 0.22     | 3    | 9.98      | 0.26       |
| 1004 | 4   | 15.01    | 0.32     | 4    | 15.02     | 0.34       |
| 1005 | 6   | 24.99    | 0.56     | 5    | 20.1      | 0.45       |
| 1006 | 7   | 29.94    | 0.66     | 6    | 25.04     | 0.65       |
| 1007 | 8   | 35.02    | 0.8      | 7    | 30.04     | 0.74       |
| 1008 | 9   | 39.98    | 0.95     | 8    | 35.03     | 0.85       |
| 1009 | 10  | 44.9     | 1.08     | 9    | 40.02     | 0.98       |
| 1010 | 11  | 49.96    | 1.22     | 10   | 45.04     | 1.13       |
| 1011 | 12  | 55.01    | 1.37     | 11   | 49.98     | 1.31       |
| 1012 | 13  | 59.95    | 1.53     | 12   | 55.07     | 1.45       |
| 1013 | 14  | 64.9     | 1.66     | 13   | 60.03     | 1.57       |
| 1014 | 15  | 69.93    | 1.8      | 14   | 65.04     | 1.73       |
| 1015 | 16  | 75.08    | 1.93     | 15   | 69.96     | 1.89       |
| 1016 | 17  | 79.91    | 2.06     | 16   | 75.15     | 2          |
| 1017 | 18  | 84.92    | 2.18     | 17   | 79.99     | 2.14       |
| 1018 | 19  | 89.89    | 2.31     | 18   | 84.92     | 2.27       |
| 1019 | 20  | 94.91    | 2.48     | 19   | 89.92     | 2.38       |
| 1020 | 21  | 99.91    | 2.64     | 20   | 94.9      | 2.56       |
| 1021 | 22  | 104.96   | 2.84     | 21   | 99.96     | 2.69       |
| 1022 | 23  | 109.99   | 3.03     | 22   | 105.01    | 2.88       |
| 1023 | 24  | 114.98   | 3.22     | 23   | 110.19    | 3.12       |
| 1024 | 25  | 119.91   | 3.39     | 24   | 115.08    | 3.34       |
| 1025 | 26  | 124.98   | 3.56     | 25   | 119.85    | 3.51       |
| 1026 | 27  | 129.97   | 3.73     | 26   | 124.9     | 3.67       |
| 1027 | 28  | 134.82   | 3.89     | 27   | 130.05    | 3.89       |
| 1028 | 29  | 139.91   | 4.05     | 28   | 134.84    | 4.05       |
| 1029 | 30  | 144.97   | 4.2      | 29   | 139.82    | 4.22       |
| 1030 | 31  | 149.92   | 4.35     | 30   | 144.97    | 4.32       |
| 1031 | 32  | 154.98   | 4.49     | 31   | 149.95    | 4.43       |
| 1032 | 33  | 159.9    | 4.66     | 32   | 154.95    | 4.6        |
| 1033 | 34  | 164.94   | 4.83     | 33   | 159.89    | 4.74       |
| 1034 | 35  | 169.88   | 5.02     | 34   | 165.01    | 4.89       |
| 1035 | 36  | 174.92   | 5.19     | 35   | 169.74    | 5.08       |
| 1036 | 37  | 179.85   | 5.34     | 36   | 175       | 5.31       |
| 1037 | 38  | 184.92   | 5.53     | 37   | 179.94    | 5.48       |
| 1038 | 39  | 189.89   | 5.7      | 38   | 184.99    | 5.66       |
| 1039 | 40  | 194.94   | 5.86     | 39   | 189.95    | 5.81       |
| 1040 | 41  | 199.91   | 6.04     | 40   | 194.98    | 5.98       |
| 1041 | 42  | 204.87   | 6.23     | 41   | 200.01    | 6.1        |
| 1042 | 43  | 209.84   | 6.42     | 42   | 204.95    | 6.3        |
| 1043 | 44  | 214.92   | 6.61     | 43   | 209.95    | 6.48       |
| 1044 | 45  | 219.92   | 6.81     | 44   | 214.88    | 6.7        |
| 1045 | 46  | 224.92   | 7.01     | 45   | 219.98    | 6.89       |
| 1046 | 47  | 229.91   | 7.2      | 46   | 224.9     | 7.06       |
| 1047 | 48  | 234.89   | 7.4      | 47   | 230       | 7.25       |
| 1048 | 49  | 239.83   | 7.61     | 48   | 234.89    | 7.44       |
| 1049 | 50  | 244.85   | 7.82     | 49   | 239.91    | 7.72       |
| 1050 | 51  | 249.86   | 8        | 50   | 244.85    | 7.92       |
| 1051 | 52  | 254.84   | 8.18     | 51   | 249.95    | 8.12       |
| 1052 | 53  | 259.79   | 8.36     | 52   | 254.86    | 8.26       |
| 1053 | 54  | 264.81   | 8.55     | 53   | 259.84    | 8.45       |

Appendix A continued

|      |     |        |       |     |        |       |
|------|-----|--------|-------|-----|--------|-------|
| 1054 | 55  | 269.79 | 8.75  | 54  | 264.79 | 8.66  |
| 1055 | 56  | 274.78 | 9     | 55  | 269.83 | 8.85  |
| 1056 | 57  | 279.75 | 9.25  | 56  | 274.87 | 9.15  |
| 1057 | 58  | 284.82 | 9.57  | 57  | 279.78 | 9.35  |
| 1058 | 59  | 289.84 | 9.85  | 58  | 284.83 | 9.57  |
| 1059 | 60  | 294.77 | 10.09 | 59  | 289.74 | 9.8   |
| 1060 | 61  | 299.85 | 10.3  | 60  | 294.69 | 10.08 |
| 1061 | 62  | 304.86 | 10.5  | 61  | 299.97 | 10.29 |
| 1062 | 63  | 309.79 | 10.66 | 62  | 304.84 | 10.48 |
| 1063 | 64  | 314.9  | 10.83 | 63  | 309.81 | 10.65 |
| 1064 | 65  | 319.81 | 11    | 64  | 314.83 | 10.82 |
| 1065 | 66  | 324.75 | 11.19 | 65  | 319.84 | 11    |
| 1066 | 67  | 329.8  | 11.36 | 66  | 324.81 | 11.17 |
| 1067 | 68  | 334.74 | 11.52 | 67  | 329.82 | 11.37 |
| 1068 | 69  | 339.77 | 11.69 | 68  | 334.78 | 11.54 |
| 1069 | 70  | 344.82 | 11.87 | 69  | 339.82 | 11.72 |
| 1070 | 71  | 349.77 | 12.04 | 70  | 344.79 | 11.88 |
| 1071 | 72  | 354.72 | 12.2  | 71  | 349.8  | 12.03 |
| 1072 | 73  | 359.78 | 12.4  | 72  | 354.81 | 12.21 |
| 1073 | 74  | 364.72 | 12.61 | 73  | 359.9  | 12.41 |
| 1074 | 75  | 369.77 | 12.82 | 74  | 364.83 | 12.61 |
| 1075 | 76  | 374.74 | 13.04 | 75  | 369.76 | 12.82 |
| 1076 | 77  | 379.7  | 13.22 | 76  | 374.84 | 13.05 |
| 1077 | 78  | 384.68 | 13.39 | 77  | 379.7  | 13.24 |
| 1078 | 79  | 389.71 | 13.59 | 78  | 384.62 | 13.43 |
| 1079 | 80  | 394.68 | 13.75 | 79  | 389.77 | 13.62 |
| 1080 | 81  | 399.76 | 13.97 | 80  | 394.79 | 13.81 |
| 1081 | 82  | 404.75 | 14.16 | 81  | 399.72 | 13.98 |
| 1082 | 83  | 409.71 | 14.36 | 82  | 404.78 | 14.16 |
| 1083 | 84  | 414.79 | 14.56 | 83  | 409.77 | 14.34 |
| 1084 | 85  | 419.76 | 14.74 | 84  | 414.79 | 14.54 |
| 1085 | 86  | 424.72 | 14.92 | 85  | 419.72 | 14.72 |
| 1086 | 87  | 429.78 | 15.11 | 86  | 424.78 | 14.91 |
| 1087 | 88  | 434.76 | 15.3  | 87  | 429.81 | 15.1  |
| 1088 | 89  | 439.73 | 15.48 | 88  | 434.73 | 15.28 |
| 1089 | 90  | 444.7  | 15.65 | 89  | 439.73 | 15.46 |
| 1090 | 91  | 449.81 | 15.83 | 90  | 444.82 | 15.63 |
| 1091 | 92  | 454.74 | 16.03 | 91  | 449.75 | 15.82 |
| 1092 | 93  | 459.73 | 16.24 | 92  | 454.75 | 16.02 |
| 1093 | 94  | 464.74 | 16.44 | 93  | 459.78 | 16.23 |
| 1094 | 95  | 469.65 | 16.62 | 94  | 464.77 | 16.43 |
| 1095 | 96  | 474.67 | 16.8  | 95  | 469.62 | 16.62 |
| 1096 | 97  | 479.7  | 16.98 | 96  | 474.59 | 16.82 |
| 1097 | 98  | 484.62 | 17.19 | 97  | 479.67 | 17.02 |
| 1098 | 99  | 489.69 | 17.43 | 98  | 484.67 | 17.24 |
| 1099 | 100 | 494.64 | 17.61 | 99  | 489.67 | 17.47 |
| 1100 | 101 | 499.63 | 17.81 | 100 | 494.74 | 17.68 |
| 1101 | 102 | 504.62 | 17.98 | 101 | 499.66 | 17.86 |
| 1102 | 103 | 509.61 | 18.14 | 102 | 504.63 | 18.05 |
| 1103 | 104 | 514.65 | 18.3  | 103 | 509.66 | 18.22 |
| 1104 | 105 | 519.68 | 18.45 | 104 | 514.66 | 18.34 |
| 1105 | 106 | 524.7  | 18.64 | 105 | 519.62 | 18.49 |
| 1106 | 107 | 529.61 | 18.8  | 106 | 524.74 | 18.66 |
| 1107 | 108 | 534.61 | 18.99 | 107 | 529.68 | 18.85 |
| 1108 | 109 | 539.58 | 19.17 | 108 | 534.61 | 19.03 |
| 1109 | 110 | 544.58 | 19.36 | 109 | 539.71 | 19.2  |

Appendix A continued

|      |     |        |       |     |        |       |
|------|-----|--------|-------|-----|--------|-------|
| 1110 | 111 | 549.63 | 19.54 | 110 | 544.69 | 19.39 |
| 1111 | 112 | 554.6  | 19.73 | 111 | 549.67 | 19.57 |
| 1112 | 113 | 559.58 | 19.92 | 112 | 554.62 | 19.76 |
| 1113 | 114 | 564.57 | 20.09 | 113 | 559.59 | 19.93 |
| 1114 | 115 | 569.64 | 20.26 | 114 | 564.58 | 20.12 |
| 1115 | 116 | 574.66 | 20.42 | 115 | 569.63 | 20.3  |
| 1116 | 117 | 579.64 | 20.6  | 116 | 574.69 | 20.49 |
| 1117 | 118 | 584.65 | 20.76 | 117 | 579.68 | 20.66 |
| 1118 | 119 | 589.59 | 20.92 | 118 | 584.62 | 20.83 |
| 1119 | 120 | 594.63 | 21.08 | 119 | 589.57 | 20.99 |
| 1120 | 121 | 599.66 | 21.26 | 120 | 594.61 | 21.14 |
| 1121 | 122 | 604.69 | 21.43 | 121 | 599.69 | 21.31 |
| 1122 | 123 | 609.6  | 21.58 | 122 | 604.68 | 21.48 |
| 1123 | 124 | 614.65 | 21.75 | 123 | 609.58 | 21.64 |
| 1124 | 125 | 619.61 | 21.92 | 124 | 614.65 | 21.79 |
| 1125 | 126 | 624.6  | 22.09 | 125 | 619.64 | 21.97 |
| 1126 | 127 | 629.65 | 22.26 | 126 | 624.67 | 22.13 |
| 1127 | 128 | 634.69 | 22.42 | 127 | 629.67 | 22.29 |
| 1128 | 129 | 639.66 | 22.58 | 128 | 634.65 | 22.45 |
| 1129 | 130 | 644.58 | 22.73 | 129 | 639.64 | 22.6  |
| 1130 | 131 | 649.56 | 22.89 | 130 | 644.68 | 22.75 |
| 1131 | 132 | 654.62 | 23.04 | 131 | 649.63 | 22.92 |
| 1132 | 133 | 659.51 | 23.22 | 132 | 654.64 | 23.07 |
| 1133 | 134 | 664.57 | 23.37 | 133 | 659.58 | 23.21 |
| 1134 | 135 | 669.56 | 23.54 | 134 | 664.7  | 23.38 |
| 1135 | 136 | 674.59 | 23.69 | 135 | 669.59 | 23.54 |
| 1136 | 137 | 679.62 | 23.84 | 136 | 674.63 | 23.7  |
| 1137 | 138 | 684.56 | 24.01 | 137 | 679.63 | 23.87 |
| 1138 | 139 | 689.54 | 24.18 | 138 | 684.59 | 24.04 |
| 1139 | 140 | 694.59 | 24.31 | 139 | 689.46 | 24.21 |
| 1140 | 141 | 699.58 | 24.49 | 140 | 694.68 | 24.37 |
| 1141 | 142 | 704.57 | 24.62 | 141 | 699.71 | 24.52 |
| 1142 | 143 | 709.57 | 24.77 | 142 | 704.67 | 24.69 |
| 1143 | 144 | 714.61 | 24.95 | 143 | 709.6  | 24.82 |
|      |     |        |       | 144 | 714.63 | 24.96 |

Note: FFID is the field file identification number. Distance and elevation are in meters. SP refers to shot point. Geo refers to geophone.

**Appendix B**  
**Cherry Valley Line 6**

| FFID | SP# | SP Dist. | SP Elev. | Geo.# | Geo Dist. | Geo. Elev. |
|------|-----|----------|----------|-------|-----------|------------|
| 1001 | 76  | 375      | 0        | 1     | 0         | 0          |
| 1002 | 77  | 380.22   | 0.1      | 2     | 5         | 0          |
| 1003 | 78  | 385.05   | 0.21     | 3     | 10        | 0          |
| 1004 | 79  | 390.01   | 0.27     | 4     | 15        | 0          |
| 1005 | 80  | 395      | 0.38     | 5     | 20        | 0          |
| 1006 | 81  | 400      | 0.48     | 6     | 25        | 0          |
| 1007 | 82  | 404.98   | 0.62     | 7     | 30        | 0          |
| 1008 | 83  | 409.83   | 0.66     | 8     | 35        | 0          |
| 1009 | 84  | 414.93   | 0.75     | 9     | 40        | 0          |
| 1010 | 85  | 420.08   | 0.83     | 10    | 45        | 0          |

Appendix B cont.

|      |     |        |      |    |     |   |
|------|-----|--------|------|----|-----|---|
| 1011 | 86  | 424.97 | 1.03 | 11 | 50  | 0 |
| 1012 | 87  | 430.04 | 1.19 | 12 | 55  | 0 |
| 1013 | 88  | 434.93 | 1.39 | 13 | 60  | 0 |
| 1014 | 89  | 439.78 | 1.85 | 14 | 65  | 0 |
| 1015 | 90  | 444.88 | 1.62 | 15 | 70  | 0 |
| 1016 | 91  | 449.85 | 1.76 | 16 | 75  | 0 |
| 1017 | 92  | 454.94 | 1.81 | 17 | 80  | 0 |
| 1018 | 93  | 459.85 | 2.14 | 18 | 85  | 0 |
| 1019 | 94  | 464.98 | 2.24 | 19 | 90  | 0 |
| 1020 | 95  | 469.89 | 2.47 | 20 | 95  | 0 |
| 1021 | 96  | 474.93 | 2.53 | 21 | 100 | 0 |
| 1022 | 98  | 484.92 | 2.82 | 22 | 105 | 0 |
| 1023 | 99  | 489.85 | 2.97 | 23 | 110 | 0 |
| 1024 | 100 | 494.84 | 3.09 | 24 | 115 | 0 |
| 1025 | 101 | 499.86 | 3.07 | 25 | 120 | 0 |
| 1026 | 102 | 504.89 | 3.32 | 26 | 125 | 0 |
| 1027 | 103 | 509.92 | 3.43 | 27 | 130 | 0 |
| 1028 | 104 | 514.92 | 3.52 | 28 | 135 | 0 |
| 1029 | 105 | 519.84 | 3.6  | 29 | 140 | 0 |
| 1030 | 106 | 524.87 | 3.76 | 30 | 145 | 0 |
| 1031 | 107 | 529.82 | 3.91 | 31 | 150 | 0 |
| 1032 | 108 | 534.91 | 3.98 | 32 | 155 | 0 |
| 1033 | 109 | 539.98 | 4.15 | 33 | 160 | 0 |
| 1034 | 110 | 544.85 | 4.33 | 34 | 165 | 0 |
| 1035 | 111 | 549.96 | 4.4  | 35 | 170 | 0 |
| 1036 | 112 | 554.9  | 4.57 | 36 | 175 | 0 |
| 1037 | 113 | 559.85 | 4.77 | 37 | 180 | 0 |
| 1038 | 114 | 564.87 | 4.77 | 38 | 185 | 0 |
| 1039 | 115 | 569.98 | 4.76 | 39 | 190 | 0 |
| 1040 | 116 | 574.89 | 4.79 | 40 | 195 | 0 |
| 1041 | 117 | 579.95 | 5.25 | 41 | 200 | 0 |
| 1042 | 118 | 584.98 | 5.36 | 42 | 205 | 0 |
| 1043 | 119 | 589.95 | 5.14 | 43 | 210 | 0 |
| 1044 | 120 | 595    | 5.42 | 44 | 215 | 0 |
| 1045 | 121 | 599.98 | 5.61 | 45 | 220 | 0 |
| 1046 | 122 | 604.91 | 5.66 | 46 | 225 | 0 |
| 1047 | 123 | 609.96 | 6.06 | 47 | 230 | 0 |
| 1048 | 124 | 614.95 | 6.12 | 48 | 235 | 0 |
| 1049 | 125 | 620.02 | 6.21 | 49 | 240 | 0 |
| 1050 | 126 | 624.9  | 6.3  | 50 | 245 | 0 |
| 1051 | 127 | 629.94 | 6.42 | 51 | 250 | 0 |
| 1052 | 128 | 635    | 6.53 | 52 | 255 | 0 |
| 1053 | 129 | 639.97 | 6.55 | 53 | 260 | 0 |
| 1054 | 130 | 645.03 | 6.72 | 54 | 265 | 0 |
| 1055 | 131 | 650.1  | 6.82 | 55 | 270 | 0 |
| 1056 | 132 | 654.99 | 7.02 | 56 | 275 | 0 |
| 1057 | 133 | 660.06 | 7.06 | 57 | 280 | 0 |
| 1058 | 134 | 664.98 | 7.2  | 58 | 285 | 0 |
| 1059 | 135 | 669.95 | 7.2  | 59 | 290 | 0 |
| 1060 | 136 | 675.01 | 7.35 | 60 | 295 | 0 |
| 1061 | 137 | 680.02 | 7.43 | 61 | 300 | 0 |
| 1062 | 138 | 685.12 | 7.72 | 62 | 305 | 0 |
| 1063 | 139 | 690.16 | 7.78 | 63 | 310 | 0 |
| 1064 | 140 | 695    | 7.86 | 64 | 315 | 0 |
| 1065 | 141 | 700.04 | 7.87 | 65 | 320 | 0 |
| 1066 | 142 | 705.1  | 8.05 | 66 | 325 | 0 |

Appendix B cont.

|      |     |        |       |     |        |       |
|------|-----|--------|-------|-----|--------|-------|
| 1067 | 143 | 710.08 | 8.07  | 67  | 330    | 0     |
| 1068 | 144 | 715.04 | 8.1   | 68  | 335    | 0     |
| 1069 | 145 | 720.09 | 8.67  | 69  | 340    | 0     |
| 1070 | 146 | 725.1  | 8.8   | 70  | 345    | 0     |
| 1071 | 147 | 730.06 | 8.96  | 71  | 350    | 0     |
| 1072 | 148 | 735.07 | 9.05  | 72  | 355    | 0     |
| 1073 | 149 | 740.06 | 9.17  | 73  | 360    | 0     |
| 1074 | 150 | 745.66 | 9.32  | 74  | 365    | 0     |
| 1075 | 151 | 749.9  | 9.43  | 75  | 370    | 0     |
| 1076 | 152 | 755.06 | 9.53  | 76  | 375.42 | -0.02 |
| 1077 | 153 | 760.1  | 9.64  | 77  | 380.22 | 0.17  |
| 1078 | 154 | 765.01 | 9.77  | 78  | 385.04 | 0.26  |
| 1079 | 155 | 770.14 | 9.92  | 79  | 389.92 | 0.26  |
| 1080 | 156 | 775.07 | 10.06 | 80  | 394.89 | 0.26  |
| 1081 | 157 | 780.1  | 10.17 | 81  | 399.93 | 0.49  |
| 1082 | 158 | 785.15 | 10.28 | 82  | 404.87 | 0.55  |
| 1083 | 159 | 790.18 | 10.41 | 83  | 409.93 | 0.82  |
| 1084 | 160 | 795.14 | 10.5  | 84  | 414.97 | 0.9   |
| 1085 | 161 | 800.14 | 10.59 | 85  | 420.06 | 0.84  |
| 1086 | 162 | 805.13 | 10.71 | 86  | 425.04 | 0.84  |
| 1087 | 163 | 810.07 | 10.23 | 87  | 429.97 | 1.19  |
| 1088 | 165 | 820.14 | 10.39 | 88  | 434.92 | 1.34  |
| 1089 | 167 | 830.13 | 10.68 | 89  | 439.79 | 1.52  |
| 1090 | 168 | 835.13 | 10.71 | 90  | 444.88 | 1.58  |
| 1091 | 169 | 840.14 | 11.03 | 91  | 449.78 | 1.76  |
| 1092 | 170 | 845.19 | 11.32 | 92  | 454.84 | 1.88  |
| 1093 | 171 | 850.18 | 11.3  | 93  | 459.83 | 2.1   |
| 1094 | 172 | 855.22 | 11.35 | 94  | 464.95 | 2.29  |
| 1095 | 173 | 860.16 | 11.53 | 95  | 469.93 | 2.43  |
| 1096 | 174 | 865.16 | 11.59 | 96  | 474.89 | 2.55  |
| 1097 | 175 | 870.15 | 11.7  | 97  | 479.77 | 2.63  |
| 1098 | 176 | 875.13 | 11.81 | 98  | 485.01 | 2.85  |
| 1099 | 177 | 880.06 | 11.9  | 99  | 489.9  | 2.85  |
| 1100 | 178 | 885.06 | 12.05 | 100 | 494.83 | 3.02  |
| 1101 | 179 | 890.1  | 12.17 | 101 | 499.85 | 3.18  |
| 1102 | 180 | 895.07 | 12.21 | 102 | 505.03 | 3.17  |
| 1103 | 181 | 900.11 | 12.3  | 103 | 509.91 | 3.41  |
| 1104 | 182 | 905.06 | 12.45 | 104 | 514.99 | 3.48  |
| 1105 | 183 | 910.09 | 12.47 | 105 | 520.01 | 3.58  |
| 1106 | 184 | 915.05 | 12.58 | 106 | 524.91 | 3.76  |
| 1107 | 185 | 920.06 | 12.62 | 107 | 529.89 | 3.85  |
| 1108 | 186 | 925.08 | 13.08 | 108 | 534.82 | 3.98  |
| 1109 | 187 | 930.01 | 13.26 | 109 | 539.95 | 4.08  |
| 1110 | 188 | 935    | 13.4  | 110 | 544.67 | 4.3   |
| 1111 | 189 | 940.08 | 13.56 | 111 | 550.01 | 4.46  |
| 1112 | 190 | 945.03 | 13.58 | 112 | 554.82 | 4.53  |
| 1113 | 191 | 950.06 | 14.22 | 113 | 559.89 | 4.69  |
| 1114 | 192 | 955.08 | 14.72 | 114 | 564.87 | 4.86  |
| 1115 | 193 | 959.99 | 15.62 | 115 | 570.05 | 4.75  |
| 1116 | 195 | 969.75 | 17.14 | 116 | 575.08 | 4.78  |
| 1117 | 196 | 974.86 | 17.26 | 117 | 579.8  | 4.93  |
| 1118 | 197 | 979.87 | 17.35 | 118 | 584.85 | 5.02  |
| 1119 | 198 | 984.79 | 17.51 | 119 | 589.92 | 5.17  |
| 1120 | 199 | 989.78 | 17.56 | 120 | 595    | 5.33  |
| 1121 | 200 | 994.79 | 17.68 | 121 | 600.03 | 5.61  |
| 1122 | 201 | 999.65 | 17.9  | 122 | 604.9  | 5.71  |

Appendix B cont.

|      |            |       |     |        |       |
|------|------------|-------|-----|--------|-------|
| 1123 | 2021004.72 | 18.14 | 123 | 609.9  | 5.97  |
| 1124 | 2041014.69 | 18.35 | 124 | 615.01 | 6.05  |
| 1125 | 2051019.69 | 18.45 | 125 | 619.89 | 6.17  |
| 1126 | 2061024.85 | 18.67 | 126 | 624.96 | 6.29  |
| 1127 | 2071029.68 | 18.82 | 127 | 630.03 | 6.43  |
| 1128 | 2081034.68 | 19.1  | 128 | 634.88 | 6.52  |
| 1129 | 2091039.67 | 19.45 | 129 | 640.02 | 6.63  |
| 1130 | 2101044.75 | 20.01 | 130 | 645.12 | 6.73  |
| 1131 | 2111049.78 | 20.22 | 131 | 649.93 | 6.86  |
| 1132 | 2121054.64 | 20.51 | 132 | 655.11 | 6.94  |
| 1133 | 2131059.61 | 19.87 | 133 | 660.08 | 7.09  |
| 1134 | 2141064.62 | 19.84 | 134 | 664.96 | 7.19  |
| 1135 | 2171079.64 | 19.91 | 135 | 670.15 | 7.12  |
| 1136 | 218 1084.8 | 20.05 | 136 | 674.99 | 7.33  |
| 1137 | 219 1089.8 | 20.07 | 137 | 680.05 | 7.52  |
| 1138 | 2201094.78 | 20.24 | 138 | 685.2  | 7.68  |
| 1139 | 2221104.74 | 20.74 | 139 | 690.19 | 7.75  |
| 1140 | 2231109.58 | 20.82 | 140 | 695.01 | 7.97  |
| 1141 | 2241114.59 | 20.94 | 141 | 700.11 | 8.03  |
| 1142 | 2251119.71 | 21.27 | 142 | 705.26 | 8.02  |
| 1143 | 2261124.88 | 21.32 | 143 | 710.19 | 8.03  |
| 1144 | 2271129.81 | 21.39 | 144 | 715.18 | 8.56  |
| 1145 | 2281134.65 | 21.66 | 145 | 720.15 | 8.65  |
| 1146 | 2291139.64 | 22.01 | 146 | 725.19 | 8.81  |
| 1147 | 230 1144.7 | 22.23 | 147 | 730.04 | 8.94  |
| 1148 | 2311149.52 | 22.52 | 148 | 735.15 | 9.04  |
| 1149 | 2321154.69 | 22.64 | 149 | 740.01 | 9.18  |
| 1150 | 2331159.68 | 22.71 | 150 | 745.22 | 9.28  |
| 1151 | 2341164.74 | 22.91 | 151 | 750.16 | 9.37  |
| 1152 | 2351169.86 | 22.95 | 152 | 755.12 | 9.48  |
| 1153 | 2361174.65 | 23.03 | 153 | 760.15 | 9.67  |
| 1154 | 2371179.68 | 23.46 | 154 | 765.1  | 9.83  |
| 1155 | 238 1184.6 | 23.54 | 155 | 770.16 | 9.92  |
| 1156 | 2401194.61 | 23.68 | 156 | 775.11 | 10.04 |
| 1157 | 2411199.68 | 23.77 | 157 | 780.17 | 10.18 |
| 1158 | 242 1204.6 | 23.88 | 158 | 785.24 | 10.29 |
| 1159 | 2431209.59 | 23.9  | 159 | 790.12 | 10.41 |
| 1160 | 2441214.61 | 24.11 | 160 | 795.31 | 10.48 |
| 1161 | 2451219.56 | 24.33 | 161 | 800.31 | 10.59 |
| 1162 | 2461224.94 | 24.53 | 162 | 805.25 | 10.69 |
| 1163 | 2471229.59 | 24.69 | 163 | 810.09 | 10.83 |
| 1164 | 2481234.58 | 24.86 | 164 | 814.9  | 10.95 |
| 1165 | 2491239.51 | 25.05 | 165 | 820    | 10.52 |
| 1166 | 2501244.52 | 25.24 | 166 | 825.24 | 10.51 |
| 1167 | 2661324.03 | 29.03 | 167 | 830.16 | 10.82 |
| 1168 | 2671329.12 | 29.16 | 168 | 835.07 | 10.76 |
| 1169 | 2681334.08 | 29.28 | 169 | 840.01 | 10.89 |
| 1170 | 2691338.82 | 29.36 | 170 | 845.17 | 11.06 |
|      |            |       | 171 | 850.19 | 11.3  |
|      |            |       | 172 | 855.16 | 11.43 |
|      |            |       | 173 | 860.05 | 11.45 |
|      |            |       | 174 | 864.84 | 11.63 |
|      |            |       | 175 | 870.01 | 11.66 |
|      |            |       | 176 | 875.18 | 11.77 |
|      |            |       | 177 | 880.13 | 11.89 |
|      |            |       | 178 | 885.16 | 11.99 |

Appendix B cont.

|     |         |       |
|-----|---------|-------|
| 179 | 890.11  | 12.13 |
| 180 | 895.18  | 12.25 |
| 181 | 900.08  | 12.36 |
| 182 | 905.19  | 12.48 |
| 183 | 910.19  | 12.54 |
| 184 | 915.04  | 12.41 |
| 185 | 920.05  | 12.5  |
| 186 | 925.06  | 12.6  |
| 187 | 930.05  | 13.45 |
| 188 | 935.11  | 13.57 |
| 189 | 940.23  | 13.65 |
| 190 | 945.05  | 13.58 |
| 191 | 950.02  | 14.18 |
| 192 | 955.08  | 14.53 |
| 193 | 960     | 15.37 |
| 194 | 964.88  | 16.79 |
| 195 | 969.73  | 17.15 |
| 196 | 974.85  | 17.26 |
| 197 | 979.78  | 17.37 |
| 198 | 984.7   | 17.42 |
| 199 | 989.76  | 17.49 |
| 200 | 994.89  | 17.6  |
| 201 | 999.62  | 17.83 |
| 202 | 1004.68 | 18.02 |
| 203 | 1009.67 | 18.24 |
| 204 | 1014.52 | 18.33 |
| 205 | 1019.73 | 18.44 |
| 206 | 1024.66 | 18.62 |
| 207 | 1029.63 | 18.81 |
| 208 | 1034.74 | 19.05 |
| 209 | 1039.59 | 19.36 |
| 210 | 1044.78 | 19.98 |
| 211 | 1049.8  | 20.23 |
| 212 | 1054.75 | 20.42 |
| 213 | 1059.84 | 19.83 |
| 214 | 1064.64 | 19.75 |
| 215 | 1069.69 | 19.77 |
| 216 | 1074.74 | 19.79 |
| 217 | 1079.79 | 19.81 |
| 218 | 1084.92 | 20.05 |
| 219 | 1089.87 | 20.09 |
| 220 | 1095.08 | 20.28 |
| 221 | 1099.95 | 20.51 |
| 222 | 1105.04 | 20.73 |
| 223 | 1109.8  | 20.85 |
| 224 | 1114.69 | 21    |
| 225 | 1119.73 | 21.25 |
| 226 | 1124.75 | 21.31 |
| 227 | 1129.73 | 21.37 |
| 228 | 1134.63 | 21.68 |
| 229 | 1139.87 | 21.92 |
| 230 | 1144.54 | 22.18 |
| 231 | 1149.48 | 22.51 |
| 232 | 1154.52 | 22.64 |
| 233 | 1159.6  | 22.76 |
| 234 | 1164.63 | 23.01 |

Appendix B cont.

|     |         |       |
|-----|---------|-------|
| 235 | 1169.85 | 22.99 |
| 236 | 1174.64 | 23.04 |
| 237 | 1179.5  | 23.4  |
| 238 | 1184.58 | 23.57 |
| 239 | 1189.74 | 23.61 |
| 240 | 1194.57 | 23.64 |
| 241 | 1199.68 | 23.7  |
| 242 | 1204.62 | 23.76 |
| 243 | 1209.84 | 23.91 |
| 244 | 1214.62 | 24.07 |
| 245 | 1219.75 | 24.29 |
| 246 | 1224.85 | 24.48 |
| 247 | 1229.73 | 24.65 |
| 248 | 1234.69 | 24.81 |
| 249 | 1239.74 | 24.99 |
| 250 | 1244.46 | 25.19 |
| 251 | 1249.7  | 23.78 |
| 252 | 1254.51 | 23.87 |
| 253 | 1259.52 | 24.11 |
| 254 | 1264.49 | 24.36 |
| 255 | 1269.53 | 24.39 |
| 256 | 1274.69 | 24.64 |
| 257 | 1279.69 | 24.84 |
| 258 | 1284.69 | 25.04 |
| 259 | 1289.69 | 25.24 |
| 260 | 1294.79 | 25.44 |
| 261 | 1299.79 | 25.64 |
| 262 | 1304.89 | 25.89 |
| 263 | 1309.66 | 26.1  |
| 264 | 1314.8  | 28.6  |
| 265 | 1318.92 | 28.85 |
| 266 | 1323.93 | 28.98 |
| 267 | 1328.98 | 29.13 |
| 268 | 1333.94 | 29.23 |
| 269 | 1338.82 | 29.36 |
| 270 | 1345    | 30    |
| 271 | 1350    | 30    |
| 272 | 1355    | 30    |
| 273 | 1360    | 30    |
| 274 | 1365    | 30    |
| 275 | 1370    | 30    |
| 276 | 1375    | 30    |
| 277 | 1380    | 30    |
| 278 | 1385    | 30    |
| 279 | 1390    | 30    |
| 280 | 1395    | 30    |
| 281 | 1400    | 30    |
| 282 | 1405    | 30    |
| 283 | 1410    | 30    |
| 284 | 1415    | 30    |
| 285 | 1420    | 30    |
| 286 | 1425    | 30    |
| 287 | 1430    | 30    |

Note: Distance and elevation are in meters. FFID refers to field file identification number. SP refers to shot point. Geo. refers to geophone.

**Appendix C**  
**Cherry Valley Line 7**

| FFID | SP# | SP Dist. | SP Elev. | Geo# | Geo Dist | Geo Elev. |
|------|-----|----------|----------|------|----------|-----------|
| 1001 | 1   | 0        | 0        | 12   | 55.08    | 1.26      |
| 1002 | 2   | 5.11     | 0.3      | 13   | 60.07    | 1.41      |
| 1003 | 3   | 10.17    | 0.6      | 14   | 64.96    | 1.51      |
| 1004 | 4   | 15.18    | 0.66     | 15   | 70.06    | 1.63      |
| 1005 | 5   | 20.2     | 0.68     | 16   | 75.14    | 1.72      |
| 1006 | 6   | 25.08    | 0.81     | 17   | 80.16    | 1.77      |
| 1007 | 7   | 30.09    | 0.89     | 18   | 85.06    | 1.89      |
| 1008 | 8   | 35.39    | 1.02     | 19   | 90.08    | 2.05      |
| 1009 | 9   | 40.25    | 0.98     | 20   | 95.22    | 2.07      |
| 1010 | 10  | 45.18    | 1.08     | 21   | 99.98    | 2.11      |
| 1011 | 11  | 50.13    | 1.12     | 22   | 105.03   | 2.25      |
| 1012 | 12  | 55.08    | 1.26     | 23   | 109.98   | 2.31      |
| 1013 | 13  | 60.07    | 1.41     | 24   | 115.07   | 2.46      |
| 1014 | 14  | 64.96    | 1.51     | 25   | 120.05   | 2.52      |
| 1015 | 15  | 70.06    | 1.63     | 26   | 125.12   | 2.63      |
| 1016 | 16  | 75.14    | 1.72     | 27   | 130.06   | 2.66      |
| 1017 | 17  | 80.16    | 1.77     | 28   | 134.85   | 2.72      |
| 1018 | 18  | 85.06    | 1.89     | 29   | 140.11   | 2.81      |
| 1019 | 19  | 90.08    | 2.05     | 30   | 145.16   | 2.98      |
| 1020 | 20  | 95.22    | 2.07     | 31   | 150.01   | 3.05      |
| 1021 | 21  | 99.98    | 2.11     | 32   | 155.07   | 3.14      |
| 1022 | 22  | 105.03   | 2.25     | 33   | 160.03   | 3.2       |
| 1023 | 23  | 109.98   | 2.31     | 34   | 164.93   | 3.31      |
| 1024 | 24  | 115.07   | 2.46     | 35   | 170.04   | 3.45      |
| 1025 | 25  | 120.05   | 2.52     | 36   | 174.95   | 3.55      |
| 1026 | 26  | 125.12   | 2.63     | 37   | 180.07   | 3.7       |
| 1027 | 27  | 130.06   | 2.66     | 38   | 185.01   | 3.88      |
| 1028 | 28  | 134.85   | 2.72     | 39   | 190.17   | 3.98      |
| 1029 | 29  | 140.11   | 2.81     | 40   | 195.25   | 4.06      |
| 1030 | 30  | 145.16   | 2.98     | 41   | 200.26   | 4.16      |
| 1031 | 31  | 150.01   | 3.05     | 42   | 205.19   | 4.24      |
| 1032 | 32  | 155.07   | 3.14     | 43   | 210.23   | 4.29      |
| 1033 | 33  | 160.03   | 3.2      | 44   | 215.24   | 4.51      |
| 1034 | 34  | 164.93   | 3.31     | 45   | 220.21   | 4.64      |
| 1035 | 35  | 170.04   | 3.45     | 46   | 225.24   | 4.71      |
| 1036 | 36  | 174.95   | 3.55     | 47   | 230.22   | 4.83      |
| 1037 | 37  | 180.07   | 3.7      | 48   | 235.24   | 5.04      |
| 1038 | 38  | 185.01   | 3.88     | 49   | 240.13   | 5.18      |
| 1039 | 39  | 190.17   | 3.98     | 50   | 245.27   | 5.3       |
| 1040 | 40  | 195.25   | 4.06     | 51   | 250.26   | 5.4       |
| 1041 | 41  | 200.26   | 4.16     | 52   | 255.26   | 5.46      |
| 1042 | 42  | 205.19   | 4.24     | 53   | 260.29   | 5.59      |
| 1043 | 43  | 210.23   | 4.29     | 54   | 265.27   | 5.72      |
| 1044 | 44  | 215.24   | 4.51     | 55   | 270.25   | 5.82      |
| 1045 | 45  | 220.21   | 4.64     | 56   | 275.28   | 5.87      |
| 1046 | 46  | 225.24   | 4.71     | 57   | 280.23   | 5.98      |
| 1047 | 47  | 230.22   | 4.83     | 58   | 285.29   | 6.06      |

Appendix C cont.

|      |     |        |       |     |        |       |
|------|-----|--------|-------|-----|--------|-------|
| 1048 | 48  | 235.24 | 5.04  | 59  | 290.2  | 6.15  |
| 1049 | 49  | 240.13 | 5.18  | 60  | 295.28 | 6.24  |
| 1050 | 50  | 245.27 | 5.3   | 61  | 300.3  | 6.34  |
| 1051 | 51  | 250.26 | 5.4   | 62  | 305.4  | 6.44  |
| 1052 | 52  | 255.26 | 5.46  | 63  | 310.5  | 6.54  |
| 1053 | 53  | 260.29 | 5.59  | 64  | 315.4  | 6.64  |
| 1054 | 54  | 265.27 | 5.72  | 65  | 320.28 | 6.69  |
| 1055 | 55  | 270.25 | 5.82  | 66  | 325.33 | 6.9   |
| 1056 | 56  | 275.28 | 5.87  | 67  | 330.29 | 6.95  |
| 1057 | 57  | 280.23 | 5.98  | 68  | 335.29 | 7.11  |
| 1058 | 58  | 285.29 | 6.06  | 69  | 340.37 | 7.26  |
| 1059 | 59  | 290.2  | 6.15  | 70  | 345.29 | 7.39  |
| 1060 | 60  | 295.28 | 6.24  | 71  | 350.34 | 7.52  |
| 1061 | 66  | 325.33 | 6.9   | 72  | 355.43 | 7.55  |
| 1062 | 67  | 330.29 | 6.95  | 73  | 360.3  | 7.79  |
| 1063 | 68  | 335.29 | 7.11  | 74  | 365.4  | 7.85  |
| 1064 | 69  | 340.37 | 7.26  | 75  | 370.31 | 7.96  |
| 1065 | 70  | 345.29 | 7.39  | 76  | 375.43 | 8.1   |
| 1066 | 71  | 350.17 | 7.44  | 77  | 380.27 | 8.21  |
| 1067 | 72  | 355.37 | 7.48  | 78  | 385.35 | 8.32  |
| 1068 | 73  | 360.21 | 7.68  | 79  | 390.19 | 8.42  |
| 1069 | 74  | 365.24 | 7.87  | 80  | 395.29 | 8.54  |
| 1070 | 75  | 370.25 | 7.91  | 81  | 400.11 | 8.64  |
| 1071 | 76  | 375.24 | 8     | 82  | 405.27 | 8.8   |
| 1072 | 77  | 380.27 | 8.19  | 83  | 410.34 | 8.84  |
| 1073 | 78  | 385.2  | 8.27  | 84  | 415.22 | 8.96  |
| 1074 | 79  | 390.25 | 8.45  | 85  | 420.21 | 9.04  |
| 1075 | 80  | 395.4  | 8.54  | 86  | 425.17 | 9.22  |
| 1076 | 81  | 400.35 | 8.69  | 87  | 430.09 | 9.25  |
| 1077 | 82  | 405.27 | 8.76  | 88  | 435.1  | 9.43  |
| 1078 | 83  | 410.3  | 8.86  | 89  | 440.34 | 9.52  |
| 1079 | 84  | 415.15 | 9.01  | 90  | 445.27 | 9.73  |
| 1080 | 85  | 420.26 | 9.03  | 91  | 450.2  | 9.85  |
| 1081 | 86  | 425.18 | 9.15  | 92  | 455.15 | 9.95  |
| 1082 | 87  | 430.31 | 9.32  | 93  | 460.22 | 10.05 |
| 1083 | 88  | 435.22 | 9.41  | 94  | 465.36 | 10.1  |
| 1084 | 89  | 440.15 | 9.55  | 95  | 470.33 | 10.19 |
| 1085 | 90  | 445.15 | 9.68  | 96  | 475.28 | 10.32 |
| 1086 | 91  | 450.23 | 9.8   | 97  | 480.16 | 10.47 |
| 1087 | 92  | 455.23 | 9.91  | 98  | 485.03 | 10.61 |
| 1088 | 93  | 460.1  | 10.02 | 99  | 490.18 | 10.67 |
| 1089 | 94  | 465.18 | 10.21 | 100 | 495.19 | 10.86 |
| 1090 | 95  | 470.14 | 10.12 | 101 | 500.24 | 11.05 |
| 1091 | 96  | 475.11 | 10.01 | 102 | 505.22 | 11.23 |
| 1092 | 97  | 480.19 | 10.43 | 103 | 510.22 | 11.22 |
| 1093 | 98  | 485.18 | 10.53 | 104 | 515.31 | 11.34 |
| 1094 | 99  | 489.95 | 10.85 | 105 | 520.2  | 11.48 |
| 1095 | 100 | 495.18 | 10.77 | 106 | 525.02 | 11.61 |
| 1096 | 101 | 500.19 | 10.8  | 107 | 530.15 | 11.72 |
| 1097 | 102 | 505.25 | 11.01 | 108 | 535.16 | 11.8  |
| 1098 | 103 | 510.31 | 11.14 | 109 | 540.2  | 11.88 |
| 1099 | 104 | 515.18 | 11.18 | 110 | 545.23 | 12    |
| 1100 | 105 | 520.25 | 11.31 | 111 | 550.24 | 12.16 |
| 1101 | 106 | 525.29 | 11.46 | 112 | 555.15 | 12.27 |
| 1102 | 107 | 530.24 | 11.7  | 113 | 560.43 | 12.4  |
| 1103 | 108 | 535.13 | 11.7  | 114 | 565.36 | 12.5  |

Appendix C cont.

|      |     |        |       |     |        |       |
|------|-----|--------|-------|-----|--------|-------|
| 1104 | 109 | 540.17 | 11.82 | 115 | 570.23 | 12.61 |
| 1105 | 110 | 545.17 | 11.94 | 116 | 575.22 | 12.84 |
| 1106 | 111 | 550.19 | 12.05 | 117 | 580.36 | 12.91 |
| 1107 | 112 | 555.14 | 12.26 | 118 | 585.21 | 13.09 |
| 1108 | 113 | 560.35 | 12.33 | 119 | 590.27 | 13.24 |
| 1109 | 114 | 565.2  | 12.49 | 120 | 595.21 | 13.32 |
| 1110 | 115 | 570.2  | 12.65 | 121 | 600.26 | 13.38 |
| 1111 | 116 | 575.26 | 12.68 | 122 | 605.18 | 13.55 |
| 1112 | 117 | 580.26 | 12.86 | 123 | 610.4  | 13.64 |
| 1113 | 118 | 585.21 | 12.99 | 124 | 615.3  | 13.8  |
| 1114 | 119 | 590.19 | 13.16 | 125 | 620.33 | 13.84 |
| 1115 | 120 | 595.17 | 13.22 | 126 | 625.2  | 14.01 |
| 1116 | 121 | 600.23 | 13.38 | 127 | 630.39 | 14.1  |
| 1117 | 122 | 605.19 | 13.5  | 128 | 635.17 | 14.4  |
| 1118 | 123 | 610.33 | 13.59 | 129 | 640.35 | 14.31 |
| 1119 | 124 | 615.3  | 13.75 | 130 | 645.32 | 14.48 |
| 1120 | 125 | 620.11 | 13.83 | 131 | 650.35 | 14.59 |
| 1121 | 126 | 625.07 | 13.94 | 132 | 655.21 | 14.68 |
| 1122 | 127 | 630.18 | 14.06 | 133 | 660.28 | 14.79 |
| 1123 | 128 | 635.17 | 14.15 | 134 | 665.25 | 14.93 |
| 1124 | 129 | 640.23 | 14.27 | 135 | 670.1  | 15.06 |
| 1125 | 130 | 645.23 | 14.38 | 136 | 675.24 | 15.19 |
| 1126 | 131 | 650.22 | 14.5  | 137 | 680.13 | 15.32 |
| 1127 | 132 | 655.2  | 14.59 | 138 | 685.28 | 15.5  |
| 1128 | 133 | 660.26 | 14.72 | 139 | 690.24 | 15.62 |
| 1129 | 134 | 665.14 | 14.85 | 140 | 695.23 | 15.77 |
| 1130 | 135 | 670.26 | 14.95 | 141 | 700.23 | 15.85 |
| 1131 | 136 | 675.19 | 15.13 | 142 | 705.27 | 15.97 |
| 1132 | 137 | 680.17 | 15.18 | 143 | 710.25 | 16.06 |
| 1133 | 138 | 685.24 | 15.43 | 144 | 715.36 | 16.12 |
| 1134 | 139 | 690.21 | 15.53 | 145 | 720.24 | 16.32 |
| 1135 | 140 | 695.24 | 15.65 | 146 | 725.08 | 16.47 |
| 1136 | 141 | 700.17 | 15.91 | 147 | 730.22 | 16.6  |
| 1137 | 142 | 705.3  | 15.99 | 148 | 735.23 | 16.68 |
| 1138 | 143 | 710.23 | 16.06 | 149 | 740.11 | 16.77 |
| 1139 | 144 | 715.24 | 16.16 | 150 | 745.18 | 16.91 |
| 1140 | 145 | 720.38 | 16.31 | 151 | 750.19 | 17.09 |
| 1141 | 146 | 725.19 | 16.44 | 152 | 755.28 | 17.13 |
| 1142 | 147 | 730.23 | 16.5  | 153 | 760.14 | 17.35 |
| 1143 | 148 | 735.21 | 16.58 | 154 | 765.09 | 17.42 |
| 1144 | 149 | 740.29 | 16.73 | 155 | 770.13 | 17.55 |
| 1145 | 150 | 745.22 | 16.84 | 156 | 775.24 | 17.63 |
| 1146 | 151 | 750.22 | 16.94 | 157 | 780.19 | 17.71 |
| 1147 | 152 | 755.27 | 17.11 | 158 | 785.18 | 17.8  |
| 1148 | 153 | 760.32 | 17.28 | 159 | 790.22 | 17.86 |
| 1149 | 154 | 765.24 | 17.39 | 160 | 795.2  | 18.02 |
| 1150 | 155 | 770.29 | 17.45 | 161 | 800.11 | 18.13 |
| 1151 | 156 | 775.22 | 17.6  | 162 | 805.17 | 18.24 |
| 1152 | 157 | 780.2  | 17.63 | 163 | 810.2  | 18.31 |
| 1153 | 158 | 785.18 | 17.78 | 164 | 815.15 | 18.44 |
| 1154 | 159 | 790.26 | 17.83 | 165 | 820.2  | 18.57 |
| 1155 | 160 | 795.24 | 17.99 | 166 | 825.32 | 18.59 |
| 1156 | 161 | 800.21 | 18.11 | 167 | 830.21 | 18.63 |
| 1157 | 162 | 805.23 | 18.18 | 168 | 835.18 | 18.82 |
| 1158 | 163 | 810.35 | 18.29 | 169 | 840.17 | 19.06 |
| 1159 | 164 | 815.32 | 18.42 | 170 | 845.25 | 19.15 |

Appendix C cont.

|      |     |         |       |     |         |       |
|------|-----|---------|-------|-----|---------|-------|
| 1160 | 165 | 820.26  | 18.47 | 171 | 850.23  | 19.17 |
| 1161 | 166 | 825.17  | 18.57 | 172 | 855.2   | 19.43 |
| 1162 | 167 | 830.18  | 18.7  | 173 | 860.2   | 19.55 |
| 1163 | 168 | 835.27  | 18.8  | 174 | 865.24  | 19.69 |
| 1164 | 169 | 840.24  | 18.92 | 175 | 870.22  | 19.77 |
| 1165 | 170 | 845.17  | 19.02 | 176 | 875.37  | 19.88 |
| 1166 | 171 | 850.25  | 19.2  | 177 | 880.23  | 20.03 |
| 1167 | 172 | 855.19  | 19.31 | 178 | 885.3   | 20.1  |
| 1168 | 173 | 860.13  | 19.5  | 179 | 890.2   | 20.18 |
| 1169 | 174 | 865.29  | 19.68 | 180 | 895.32  | 20.5  |
| 1170 | 175 | 870.22  | 19.76 | 181 | 900.4   | 20.46 |
| 1171 | 176 | 875.17  | 19.85 | 182 | 905.43  | 20.52 |
| 1172 | 177 | 880.34  | 20.06 | 183 | 910.14  | 20.57 |
| 1173 | 178 | 885.2   | 20.15 | 184 | 915.18  | 20.92 |
| 1174 | 179 | 890.24  | 20.17 | 185 | 920.31  | 21.14 |
| 1175 | 180 | 895.27  | 20.4  | 186 | 925.26  | 21.16 |
| 1176 | 181 | 900.28  | 20.53 | 187 | 930.16  | 21.36 |
| 1177 | 182 | 905.26  | 20.63 | 188 | 935.1   | 21.68 |
| 1178 | 183 | 910.12  | 20.92 | 189 | 940.21  | 21.74 |
| 1179 | 184 | 915.12  | 20.91 | 190 | 945.27  | 21.63 |
| 1180 | 185 | 920.19  | 21.15 | 191 | 950.29  | 22.1  |
| 1181 | 186 | 925.28  | 21.21 | 192 | 955.15  | 21.88 |
| 1182 | 187 | 930.27  | 21.42 | 193 | 960.01  | 21.93 |
| 1183 | 188 | 935.15  | 21.31 | 194 | 965.17  | 22.14 |
| 1184 | 189 | 940.21  | 21.49 | 195 | 970.24  | 22.06 |
| 1185 | 190 | 945.29  | 21.6  | 196 | 975.21  | 22.16 |
| 1186 | 191 | 950.22  | 21.92 | 197 | 980.26  | 22.28 |
| 1187 | 192 | 955.2   | 22.11 | 198 | 985.24  | 22.48 |
| 1188 | 193 | 960.15  | 21.94 | 199 | 990.22  | 22.58 |
| 1189 | 194 | 965.18  | 21.97 | 200 | 995.3   | 22.68 |
| 1190 | 195 | 970.24  | 22.03 | 201 | 1000.29 | 22.75 |
| 1191 | 196 | 975.21  | 22.14 | 202 | 1005.34 | 22.89 |
| 1192 | 197 | 980.22  | 22.3  | 203 | 1010.27 | 23.21 |
| 1193 | 198 | 985.25  | 22.39 | 204 | 1015.31 | 23.18 |
| 1194 | 199 | 990.28  | 22.65 | 205 | 1020.31 | 23.36 |
| 1195 | 200 | 995.21  | 22.7  | 206 | 1025.29 | 23.68 |
| 1196 | 201 | 1000.14 | 22.75 | 207 | 1030.41 | 24.01 |
| 1197 | 202 | 1005.18 | 22.85 | 208 | 1035.43 | 23.94 |
| 1198 | 203 | 1010.19 | 23.12 | 209 | 1040.57 | 24.08 |
| 1199 | 204 | 1015.19 | 23.29 | 210 | 1045.47 | 24.21 |
| 1200 | 205 | 1020.22 | 23.33 | 211 | 1050.52 | 24.31 |
| 1201 | 206 | 1025.23 | 23.56 | 212 | 1055.33 | 24.44 |
| 1202 | 207 | 1030.3  | 23.79 | 213 | 1060.26 | 24.61 |
| 1203 | 208 | 1035.26 | 24.06 | 214 | 1065.41 | 24.72 |
| 1204 | 209 | 1040.46 | 24.08 | 215 | 1070.38 | 24.85 |
| 1205 | 210 | 1045.35 | 24.19 | 216 | 1075.34 | 24.95 |
| 1206 | 211 | 1050.29 | 24.35 | 217 | 1080.47 | 25.04 |
| 1207 | 212 | 1055.29 | 24.47 | 218 | 1085.22 | 25.17 |
| 1208 | 213 | 1060.27 | 24.62 | 219 | 1090.35 | 25.37 |
| 1209 | 214 | 1065.36 | 24.72 | 220 | 1095.33 | 25.55 |
| 1210 | 215 | 1070.3  | 24.83 | 221 | 1100.44 | 25.61 |
| 1211 | 216 | 1075.24 | 24.88 | 222 | 1105.42 | 25.61 |
| 1212 | 217 | 1080.19 | 25.04 | 223 | 1110.25 | 25.74 |
| 1213 | 218 | 1085.22 | 25.32 | 224 | 1115.29 | 25.81 |
| 1214 | 219 | 1090.23 | 25.34 | 225 | 1120.28 | 25.9  |
| 1215 | 220 | 1095.26 | 25.56 | 226 | 1125.33 | 26.04 |

Appendix C cont.

|      |            |       |     |         |       |
|------|------------|-------|-----|---------|-------|
| 1216 | 2211100.31 | 25.52 | 227 | 1130.26 | 26.19 |
| 1217 | 2221105.43 | 25.56 | 228 | 1135.16 | 26.29 |
| 1218 | 223 1110.3 | 25.67 | 229 | 1140.24 | 26.41 |
| 1219 | 224 1115.3 | 25.8  | 230 | 1145.33 | 26.57 |
| 1220 | 2251120.28 | 25.94 | 231 | 1150.3  | 26.75 |
| 1221 | 2261125.21 | 26.09 | 232 | 1155.34 | 26.84 |
| 1222 | 2271130.14 | 26.17 | 233 | 1160.21 | 26.93 |
| 1223 | 2281135.17 | 26.3  | 234 | 1165.17 | 27.12 |
| 1224 | 2291140.21 | 26.41 | 235 | 1170.29 | 27.32 |
| 1225 | 2301145.21 | 26.56 | 236 | 1175.25 | 27.36 |
| 1226 | 2311150.21 | 26.71 | 237 | 1180.24 | 27.56 |
| 1227 | 2321155.17 | 26.81 | 238 | 1185.18 | 27.63 |
| 1228 | 2331160.16 | 26.91 | 239 | 1190.13 | 27.72 |
| 1229 | 234 1165.1 | 27.08 | 240 | 1195.16 | 27.86 |
| 1230 | 2351170.23 | 27.2  | 241 | 1200.21 | 27.99 |
| 1231 | 236 1175.2 | 27.32 | 242 | 1205.09 | 28.14 |
| 1232 | 2371180.16 | 27.52 | 243 | 1210.05 | 28.32 |
| 1233 | 2381185.15 | 27.6  | 244 | 1215.12 | 28.33 |
| 1234 | 2391190.09 | 27.74 | 245 | 1220.12 | 28.48 |
| 1235 | 2401195.15 | 27.83 | 246 | 1225.12 | 28.67 |
| 1236 | 2411200.12 | 27.98 | 247 | 1230.22 | 28.82 |
| 1237 | 2421205.13 | 28.16 | 248 | 1234.75 | 28.85 |
| 1238 | 2431210.05 | 28.28 | 249 | 1239.81 | 29.01 |
| 1239 | 2441215.06 | 28.36 | 250 | 1245.05 | 29.01 |
| 1240 | 2451220.06 | 28.53 | 251 | 1250.06 | 29.13 |
| 1241 | 2461225.09 | 28.68 | 252 | 1255.12 | 29.25 |
| 1242 | 247 1230.1 | 28.76 | 253 | 1260    | 29.41 |
| 1243 | 2481235.03 | 28.89 | 254 | 1265.08 | 29.54 |
| 1244 | 2491240.08 | 28.91 | 255 | 1270.1  | 29.65 |
| 1245 | 250 1245.1 | 29.15 | 256 | 1275.22 | 29.76 |
| 1246 | 2511250.07 | 29.14 | 257 | 1280.05 | 29.89 |
| 1247 | 2521255.05 | 29.3  | 258 | 1285.12 | 30.09 |
| 1248 | 2531260.07 | 29.41 | 259 | 1290.16 | 30.18 |
| 1249 | 2541265.04 | 29.57 | 260 | 1295.15 | 30.27 |
| 1250 | 2551270.06 | 29.64 | 261 | 1300.16 | 30.4  |
| 1251 | 2561275.09 | 29.79 | 262 | 1305.17 | 30.51 |
| 1252 | 2571280.11 | 29.86 | 263 | 1310.11 | 30.62 |
| 1253 | 2581285.05 | 30.05 | 264 | 1315.03 | 30.67 |
| 1254 | 2591290.13 | 30.21 | 265 | 1320.05 | 30.8  |
| 1255 | 2601295.16 | 30.28 | 266 | 1325.09 | 30.91 |
| 1256 | 2621305.09 | 30.51 | 267 | 1330.23 | 31.12 |
| 1257 | 263 1310   | 30.61 | 268 | 1335.16 | 31.28 |
| 1258 | 2641315.02 | 30.69 | 269 | 1340.19 | 31.4  |
| 1259 | 2651320.06 | 30.83 | 270 | 1345.16 | 31.48 |
| 1260 | 2661325.06 | 30.92 | 271 | 1350.21 | 31.66 |
| 1261 | 2671330.14 | 31.07 | 272 | 1355.15 | 31.78 |
| 1262 | 2681335.07 | 31.18 | 273 | 1360.2  | 31.83 |
| 1263 | 2691340.04 | 31.32 | 274 | 1365.05 | 31.94 |
| 1264 | 2701345.12 | 31.53 | 275 | 1370.24 | 32.05 |
| 1265 | 2711350.22 | 31.64 | 276 | 1375.21 | 32.18 |
| 1266 | 2721355.06 | 31.73 | 277 | 1380.21 | 32.34 |
| 1267 | 2731360.08 | 31.81 | 278 | 1385.24 | 32.47 |
| 1268 | 2741365.07 | 31.92 | 279 | 1390.15 | 32.57 |
| 1269 | 2751370.09 | 32.06 | 280 | 1395.36 | 32.69 |
| 1270 | 2761375.14 | 32.16 | 281 | 1400.28 | 32.85 |
| 1271 | 2771380.14 | 32.32 | 282 | 1405.34 | 32.95 |

Appendix C cont.

|      |            |       |     |         |       |
|------|------------|-------|-----|---------|-------|
| 1272 | 278 1385.2 | 32.44 | 283 | 1410.2  | 33.03 |
| 1273 | 2791390.23 | 32.54 | 284 | 1415.12 | 33.09 |
| 1274 | 280 1395.2 | 32.73 | 285 | 1420.17 | 33.24 |
| 1275 | 2811400.21 | 32.85 | 286 | 1425.1  | 33.36 |
| 1276 | 2821405.18 | 32.94 | 287 | 1430.09 | 33.46 |
| 1277 | 2831410.12 | 33.02 | 288 | 1435.11 | 33.51 |
| 1278 | 2841415.11 | 33.14 | 289 | 1440.18 | 33.69 |
| 1279 | 2851420.13 | 33.22 | 290 | 1445.26 | 33.81 |
| 1280 | 2861425.19 | 33.33 | 291 | 1450.19 | 33.94 |
| 1281 | 2871430.18 | 33.42 | 292 | 1455.22 | 34.02 |
| 1282 | 2881435.19 | 33.5  | 293 | 1459.94 | 34.12 |
| 1283 | 2891440.16 | 33.72 | 294 | 1464.64 | 34.26 |
| 1284 | 2901445.22 | 33.78 | 295 | 1469.5  | 34.58 |
| 1285 | 2911450.18 | 33.93 | 296 | 1474.66 | 34.82 |
| 1286 | 292 1455.2 | 34    | 297 | 1479.57 | 34.81 |
| 1287 | 293 1459.9 | 34.13 | 298 | 1484.66 | 34.97 |
| 1288 | 2941464.54 | 34.33 | 299 | 1489.61 | 35.1  |
| 1289 | 2951469.55 | 34.44 | 300 | 1494.66 | 35.22 |
| 1290 | 2961474.48 | 34.59 | 301 | 1499.49 | 35.33 |
| 1291 | 2971479.66 | 34.7  | 302 | 1504.59 | 35.47 |
| 1292 | 2981484.57 | 34.95 | 303 | 1509.56 | 35.57 |
| 1293 | 2991489.55 | 35.07 | 304 | 1514.56 | 35.7  |
| 1294 | 3001494.56 | 35.18 | 305 | 1519.64 | 35.83 |
| 1295 | 3011499.56 | 35.35 | 306 | 1524.51 | 35.89 |
| 1296 | 3021504.55 | 35.44 | 307 | 1529.37 | 36.08 |
| 1297 | 3031509.54 | 35.57 | 308 | 1534.49 | 36.17 |
| 1298 | 3041514.51 | 35.63 | 309 | 1539.55 | 36.3  |
| 1299 | 3051519.57 | 35.79 | 310 | 1544.67 | 36.44 |
| 1300 | 3061524.52 | 35.88 | 311 | 1549.4  | 36.49 |
| 1301 | 3071529.53 | 36.08 | 312 | 1554.4  | 36.65 |
| 1302 | 3081534.56 | 36.22 | 313 | 1559.37 | 36.82 |
| 1303 | 3091539.63 | 36.34 | 314 | 1564.43 | 36.91 |
| 1304 | 310 1544.6 | 36.44 | 315 | 1569.39 | 37.14 |
| 1305 | 3111549.52 | 36.58 | 316 | 1574.43 | 37.17 |
| 1306 | 3121554.56 | 36.7  | 317 | 1579.48 | 37.12 |
| 1307 | 3131559.43 | 36.87 | 318 | 1584.52 | 37.47 |
| 1308 | 3141564.44 | 37.1  | 319 | 1589.43 | 37.58 |
| 1309 | 3151569.46 | 36.96 | 320 | 1594.38 | 37.74 |
| 1310 | 3161574.52 | 37.25 | 321 | 1599.52 | 37.98 |
| 1311 | 3171579.49 | 37.41 | 322 | 1604.42 | 38.02 |
| 1312 | 3181584.56 | 37.52 | 323 | 1609.59 | 38.03 |
| 1313 | 3191589.45 | 37.63 | 324 | 1615    | 38    |
| 1314 | 3201594.34 | 37.64 | 325 | 1620    | 38    |
| 1315 | 3211599.29 | 37.94 | 326 | 1625    | 38    |
| 1316 | 3221604.43 | 37.93 | 327 | 1630    | 38    |
| 1317 | 3231609.42 | 38.05 | 328 | 1635    | 38    |
|      |            |       | 329 | 1640    | 38    |
|      |            |       | 330 | 1645    | 38    |
|      |            |       | 331 | 1650    | 38    |
|      |            |       | 332 | 1655    | 38    |
|      |            |       | 333 | 1660    | 38    |
|      |            |       | 334 | 1665    | 38    |
|      |            |       | 335 | 1670    | 38    |
|      |            |       | 336 | 1675    | 38    |
|      |            |       | 337 | 1680    | 38    |
|      |            |       | 338 | 1685    | 38    |

Appendix C cont.

|     |      |    |
|-----|------|----|
| 339 | 1690 | 38 |
| 340 | 1695 | 38 |
| 341 | 1700 | 38 |
| 342 | 1705 | 38 |
| 343 | 1710 | 38 |
| 344 | 1715 | 38 |
| 345 | 1720 | 38 |
| 346 | 1725 | 38 |
| 347 | 1730 | 38 |
| 348 | 1735 | 38 |
| 349 | 1740 | 38 |
| 350 | 1745 | 38 |
| 351 | 1750 | 38 |
| 352 | 1755 | 38 |
| 353 | 1760 | 38 |
| 354 | 1765 | 38 |
| 355 | 1770 | 38 |
| 356 | 1775 | 38 |
| 357 | 1780 | 38 |
| 358 | 1785 | 38 |
| 359 | 1790 | 38 |
| 360 | 1795 | 38 |
| 361 | 1800 | 38 |
| 362 | 1805 | 38 |
| 363 | 1810 | 38 |
| 364 | 1815 | 38 |
| 365 | 1820 | 38 |
| 366 | 1825 | 38 |
| 367 | 1830 | 38 |
| 368 | 1835 | 38 |
| 369 | 1840 | 38 |
| 370 | 1845 | 38 |
| 371 | 1850 | 38 |
| 372 | 1855 | 38 |
| 373 | 1860 | 38 |
| 374 | 1865 | 38 |
| 375 | 1870 | 38 |
| 376 | 1875 | 38 |
| 377 | 1880 | 38 |
| 378 | 1885 | 38 |
| 379 | 1890 | 38 |
| 380 | 1895 | 38 |
| 381 | 1900 | 38 |
| 382 | 1905 | 38 |
| 383 | 1910 | 38 |
| 384 | 1915 | 38 |
| 385 | 1920 | 38 |
| 386 | 1925 | 38 |
| 387 | 1930 | 38 |
| 388 | 1935 | 38 |
| 389 | 1940 | 38 |
| 390 | 1945 | 38 |
| 391 | 1950 | 38 |
| 392 | 1955 | 38 |
| 393 | 1960 | 38 |
| 394 | 1965 | 38 |

Appendix C cont.

|     |      |    |
|-----|------|----|
| 395 | 1970 | 38 |
| 396 | 1975 | 38 |
| 397 | 1980 | 38 |
| 398 | 1985 | 38 |
| 399 | 1990 | 38 |
| 400 | 1995 | 38 |
| 401 | 2000 | 38 |
| 402 | 2005 | 38 |
| 403 | 2010 | 38 |
| 404 | 2015 | 38 |
| 405 | 2020 | 38 |
| 406 | 2025 | 38 |
| 407 | 2030 | 38 |
| 408 | 2035 | 38 |
| 409 | 2040 | 38 |
| 410 | 2045 | 38 |
| 411 | 2050 | 38 |
| 412 | 2055 | 38 |
| 413 | 2060 | 38 |

Note: FFID is the field file identification number. Distance and elevation are in meters. SP refers to shot point. Geo refers to geophone.

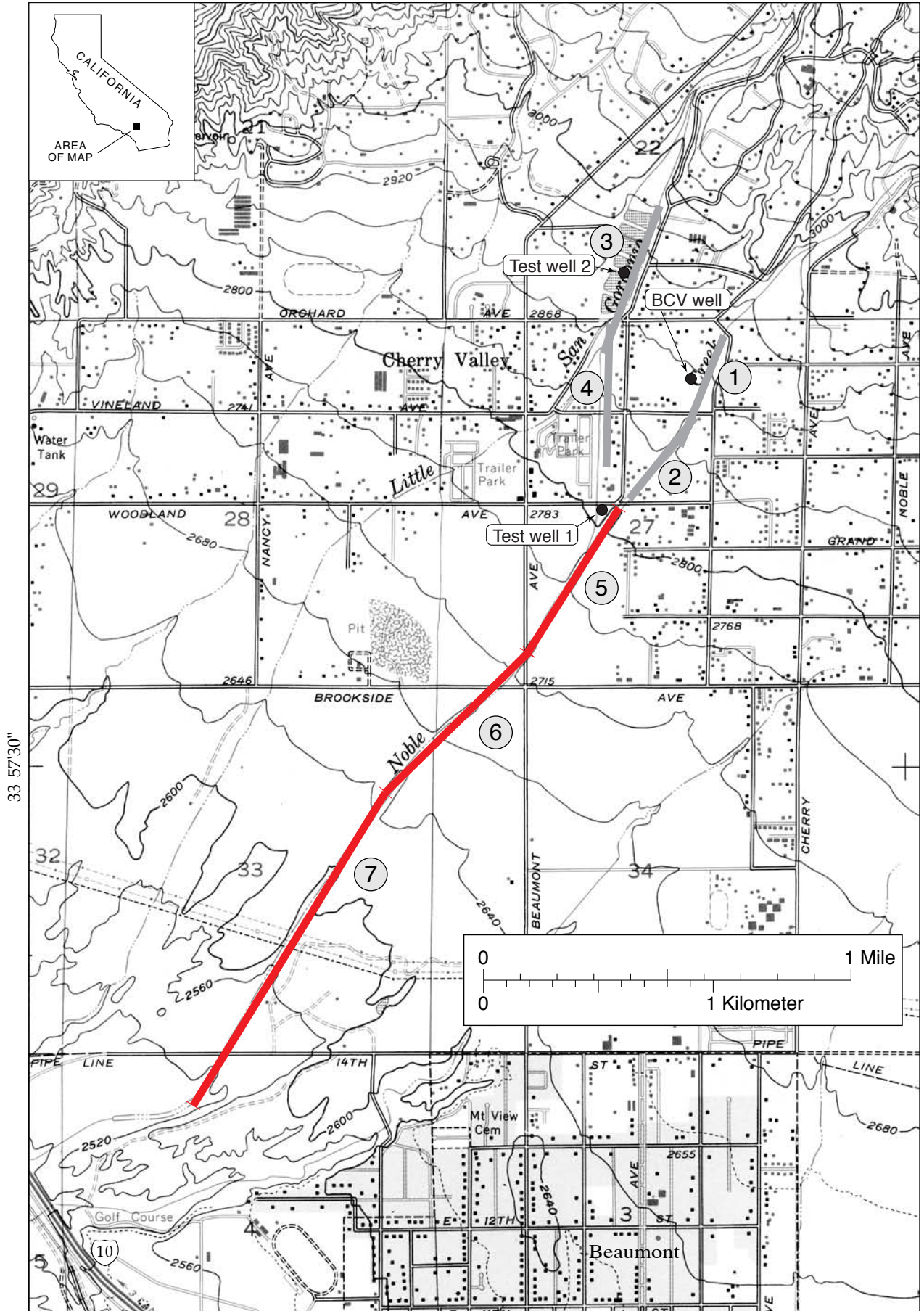


Figure 1a



116°45'

116°30'

116°15'

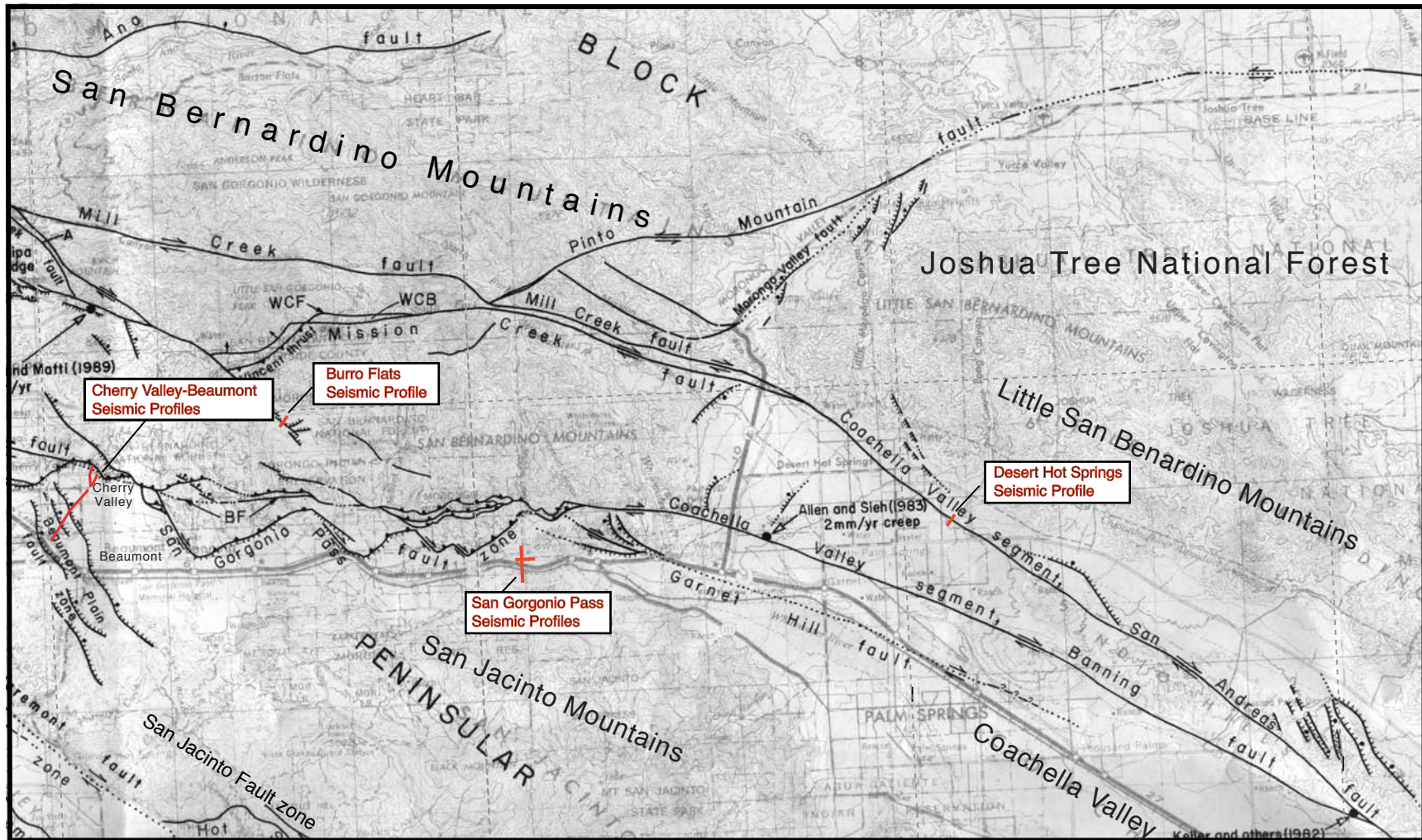


Figure 1b

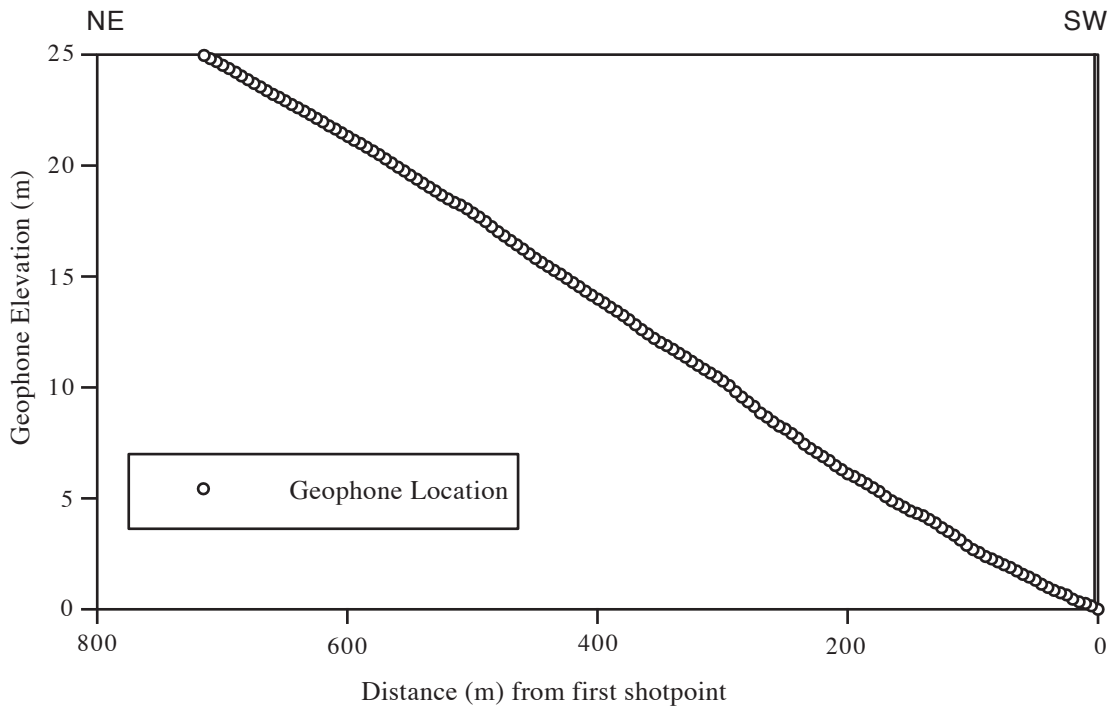


Figure 2

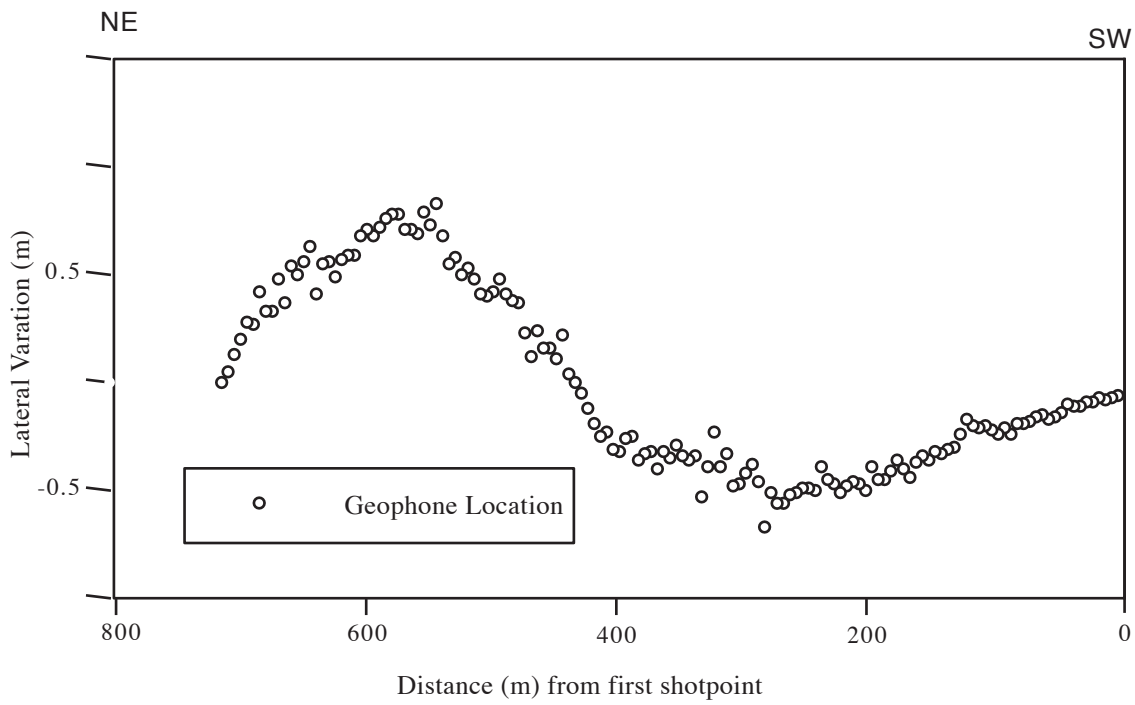


Figure.3

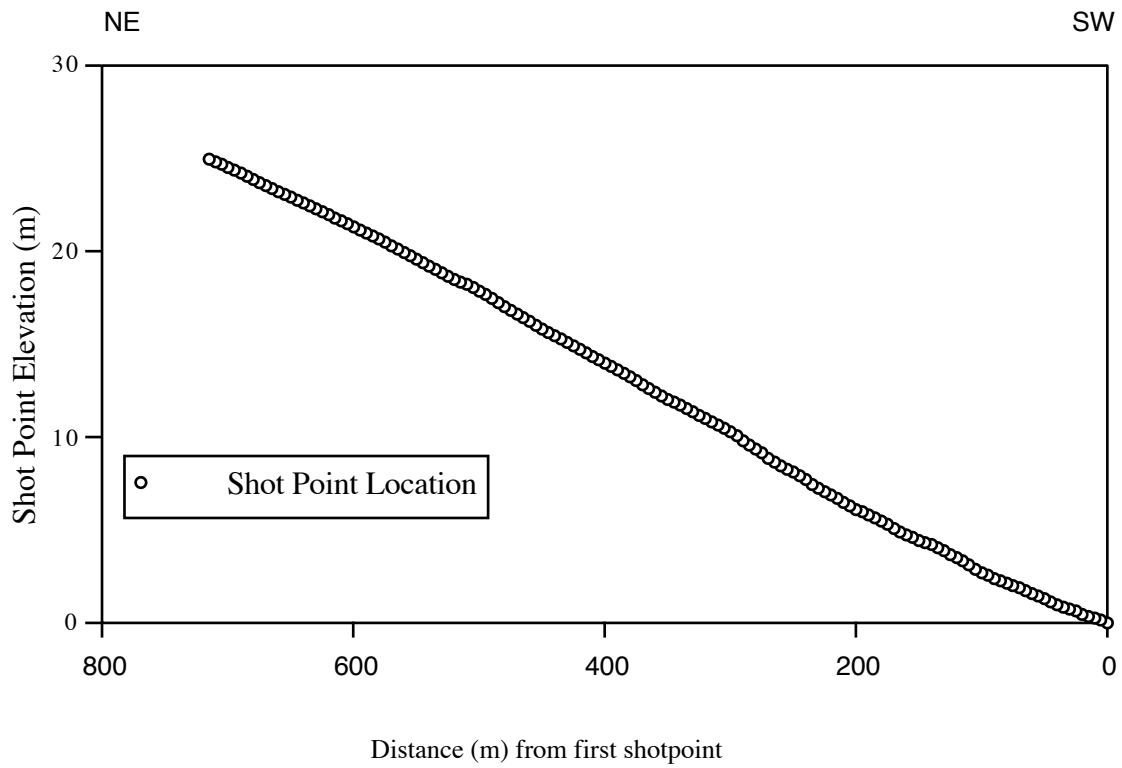


Figure. 4

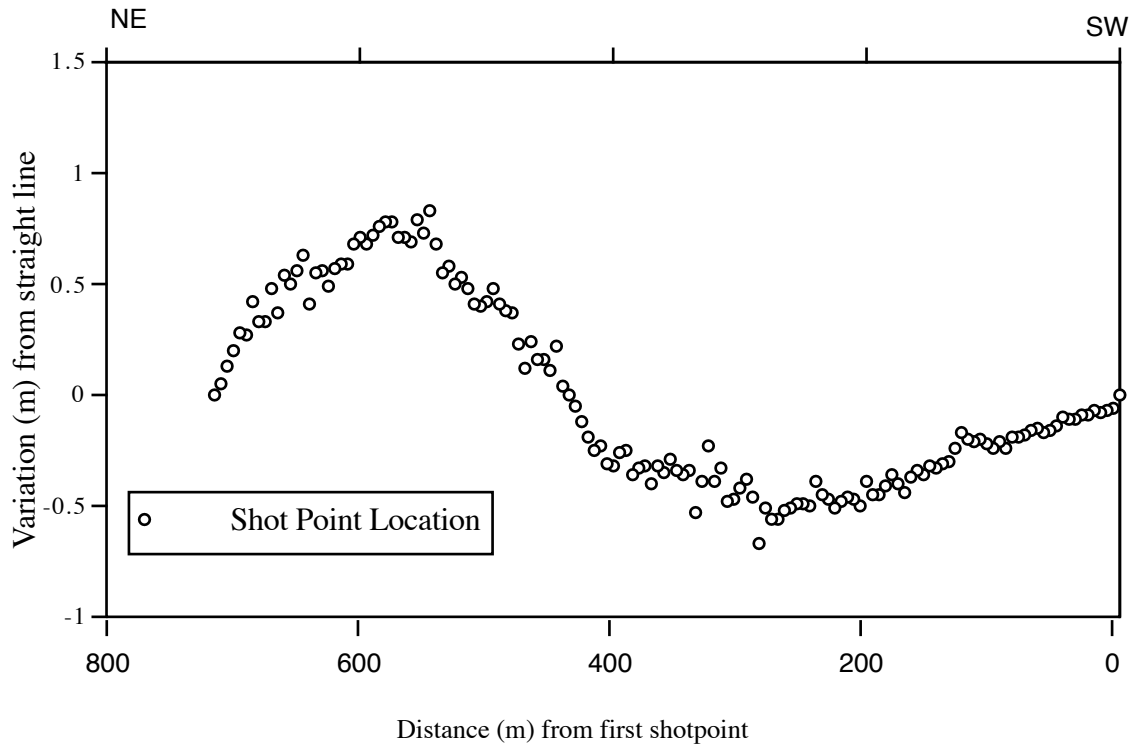


Figure. 5

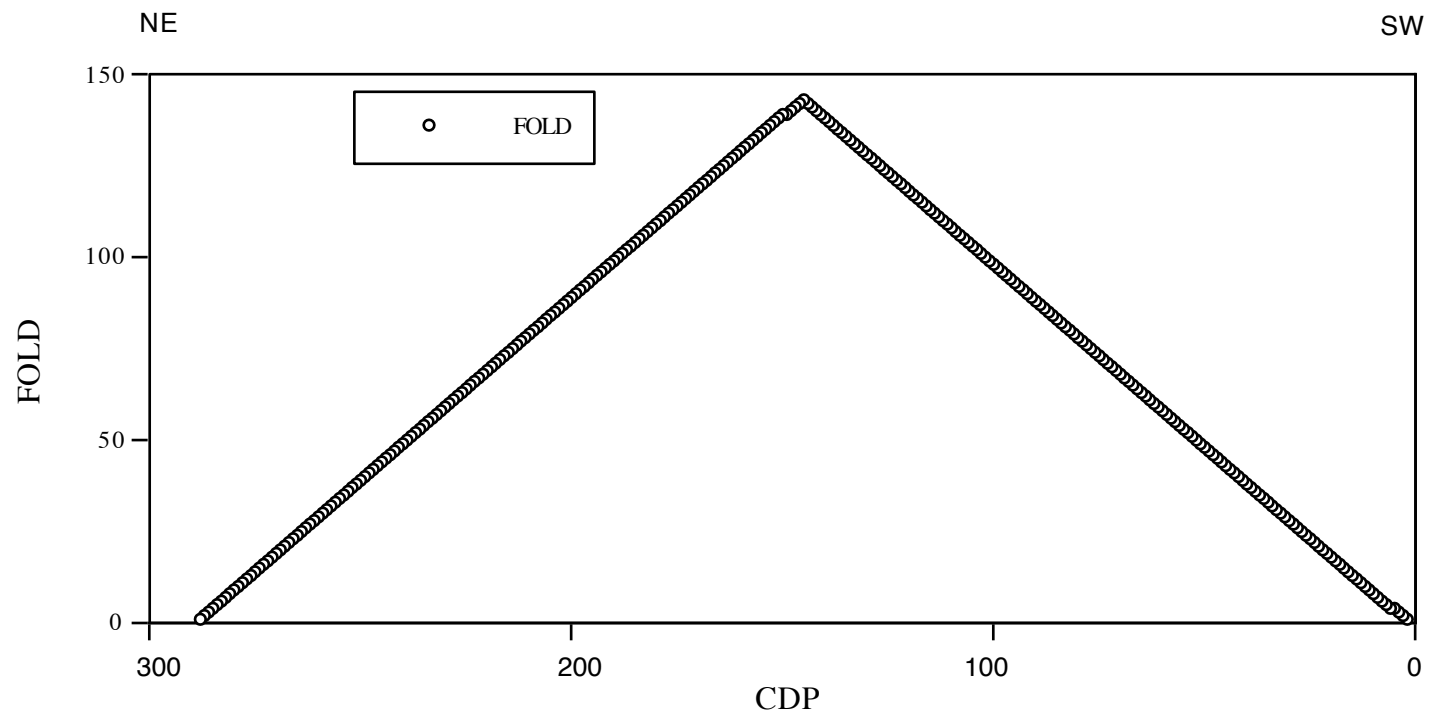


Figure 6

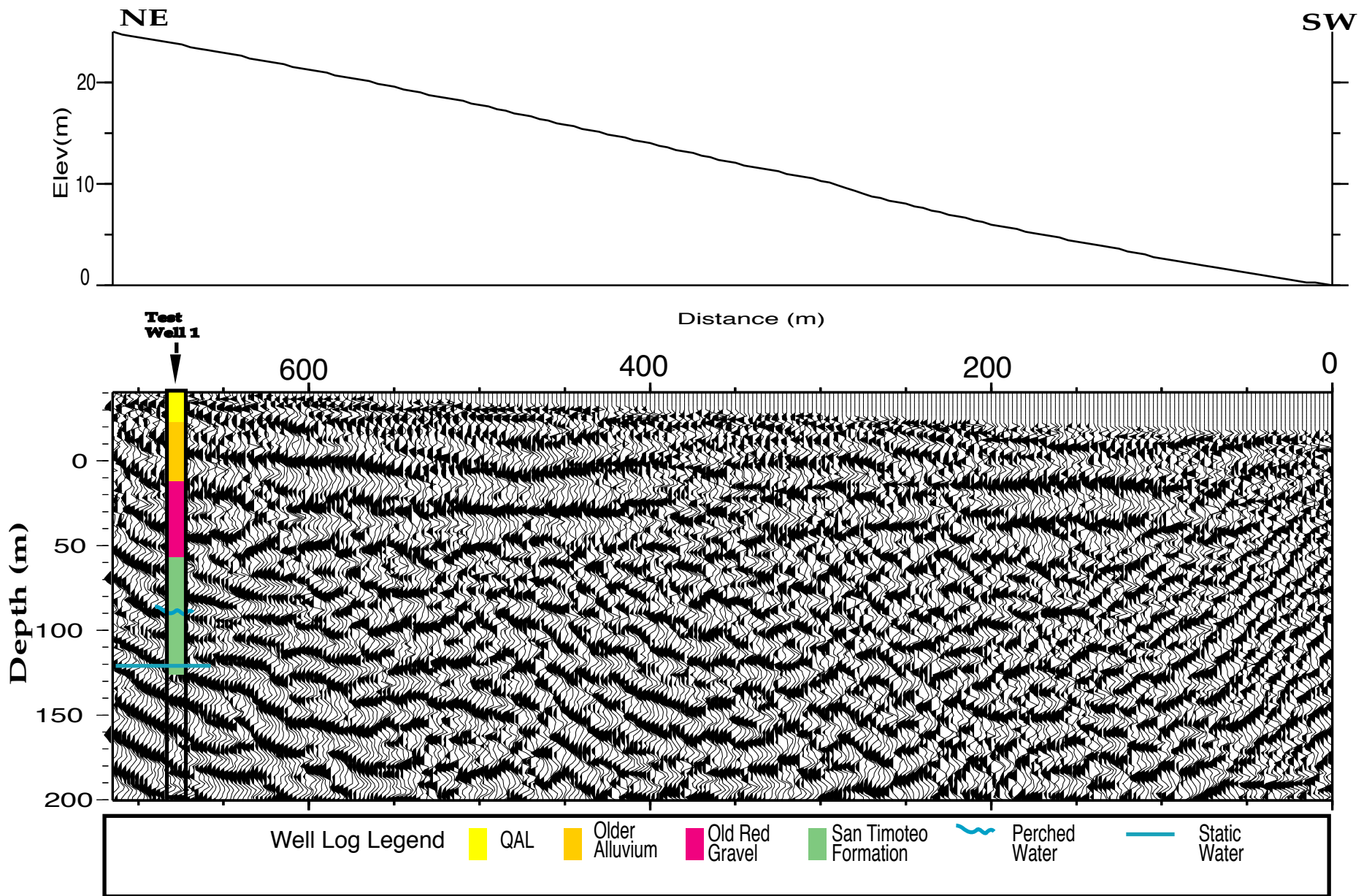


Figure. 7

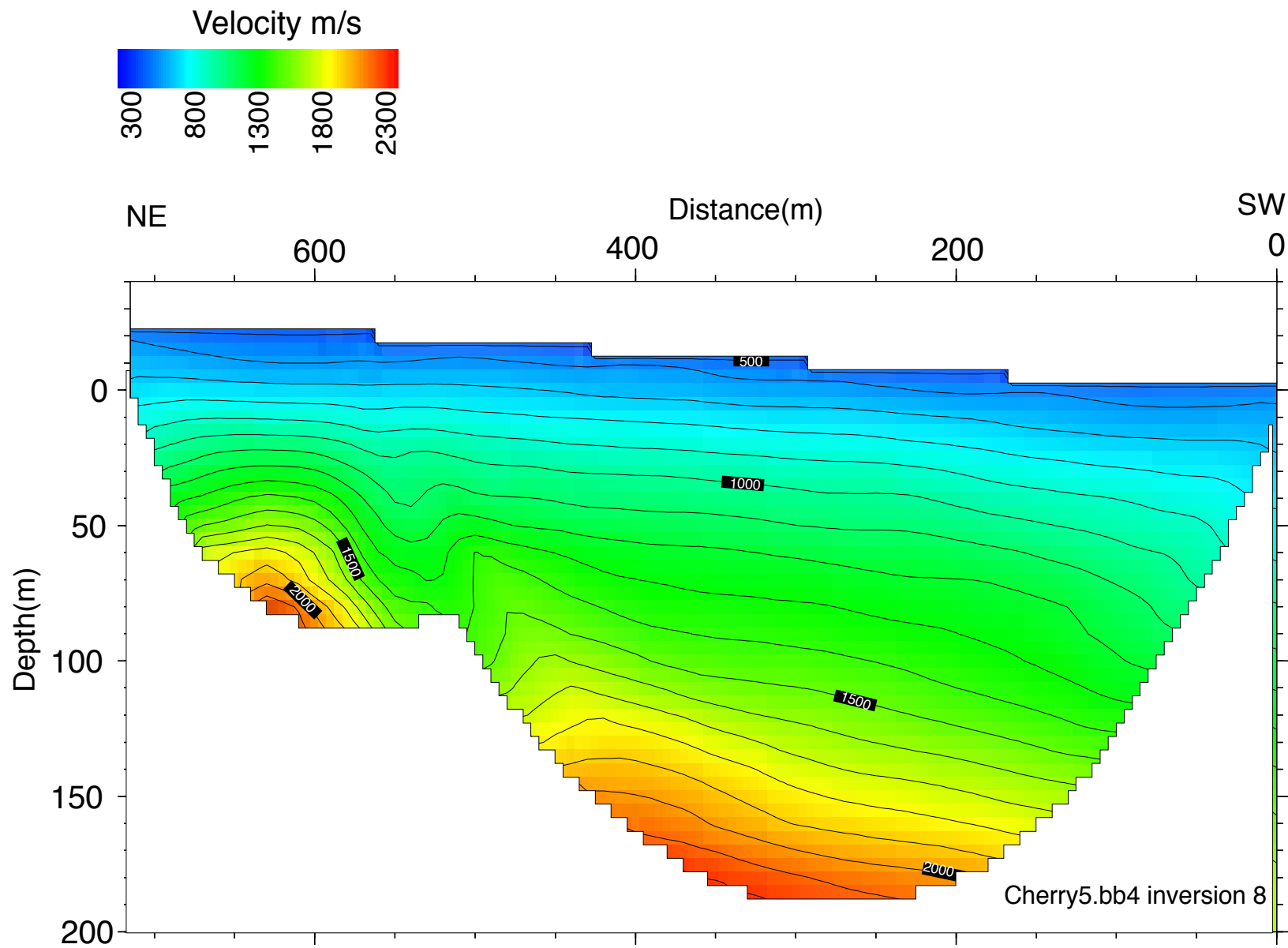


Figure 8

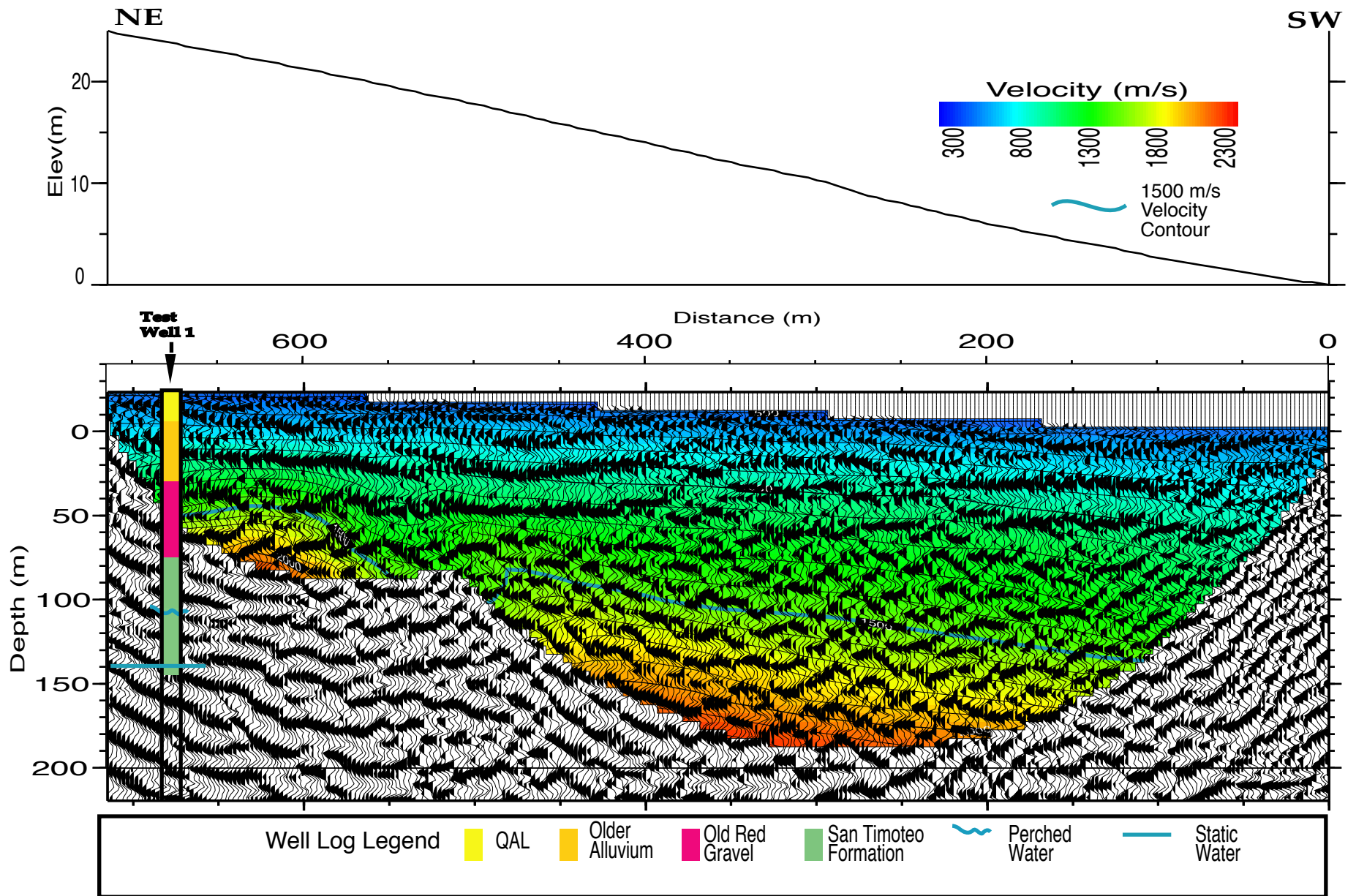


Figure. 9

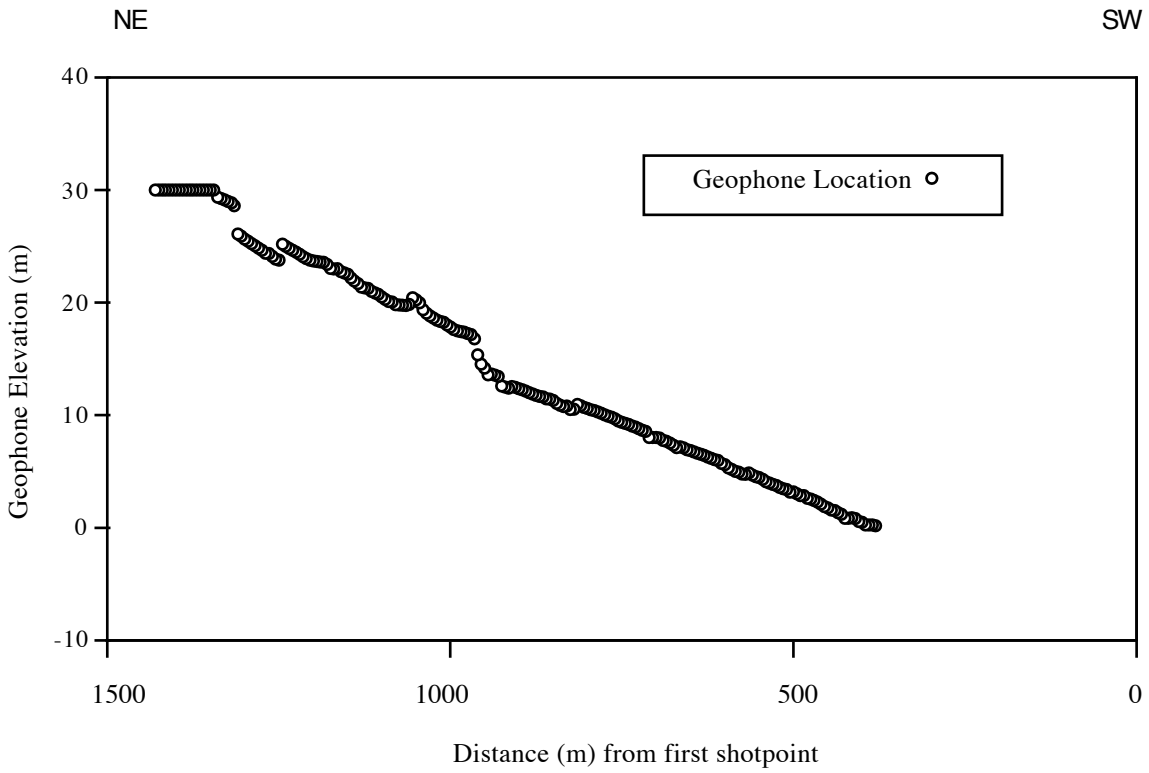


Figure 10

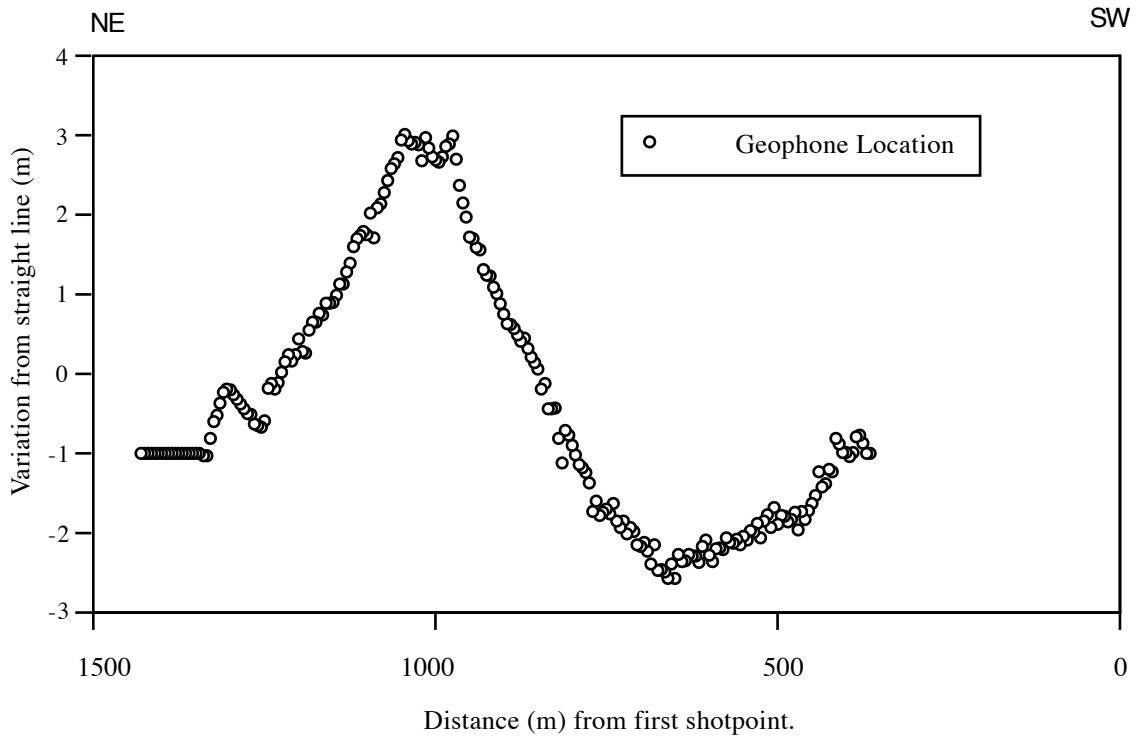


Figure 11

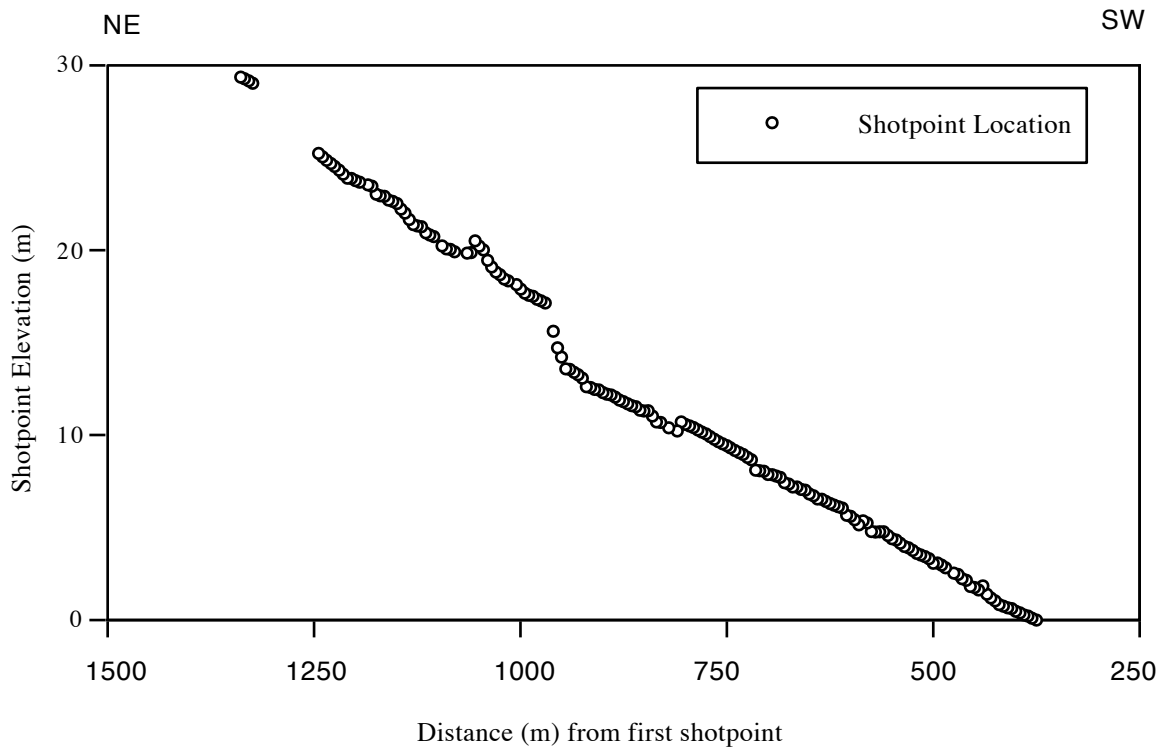


Figure 12

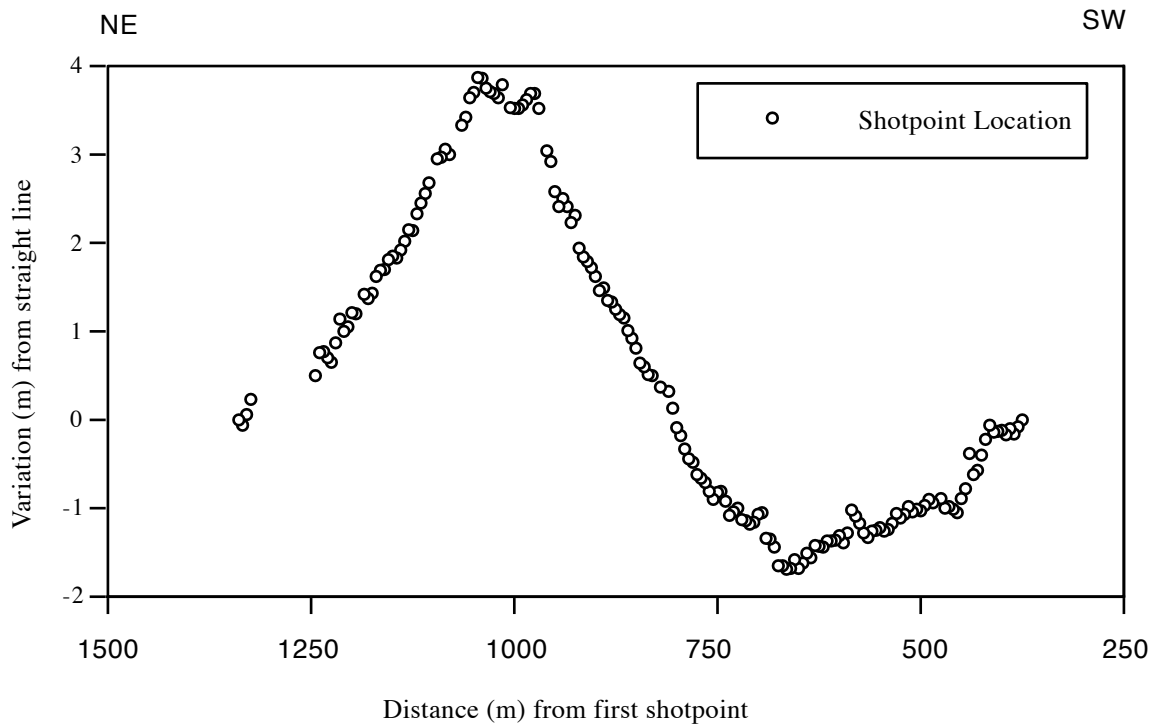


Figure 13

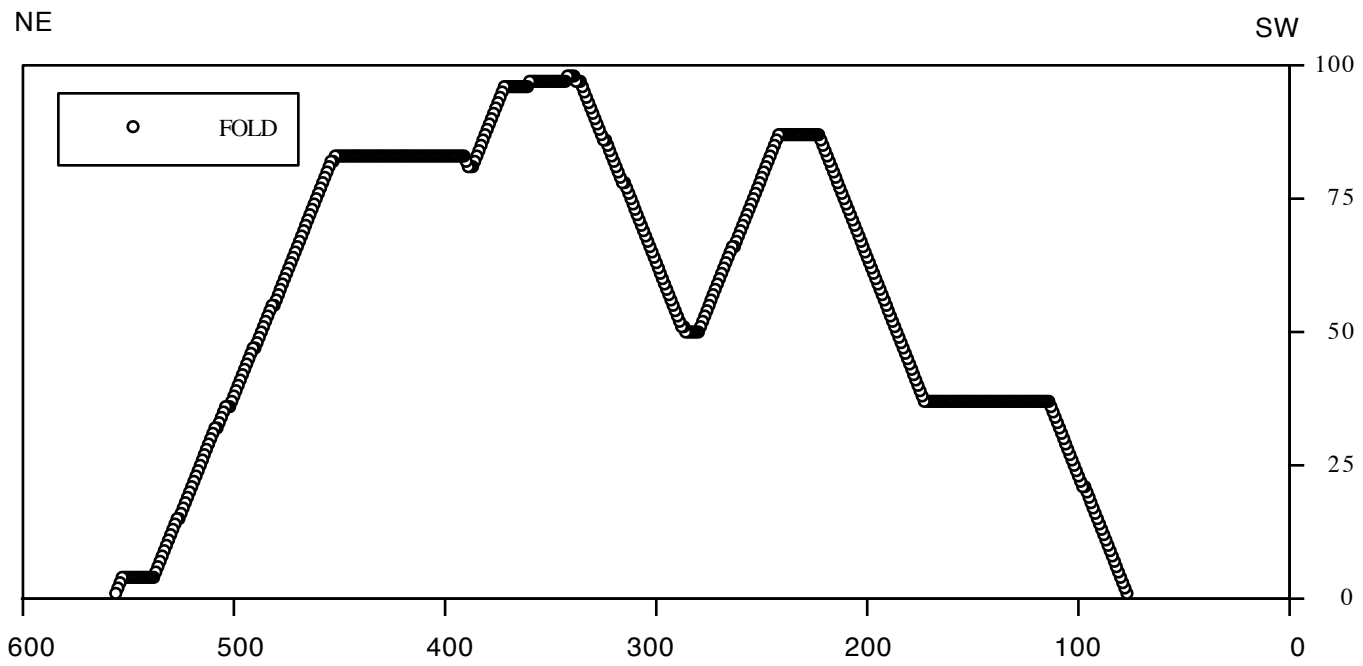


Figure 14

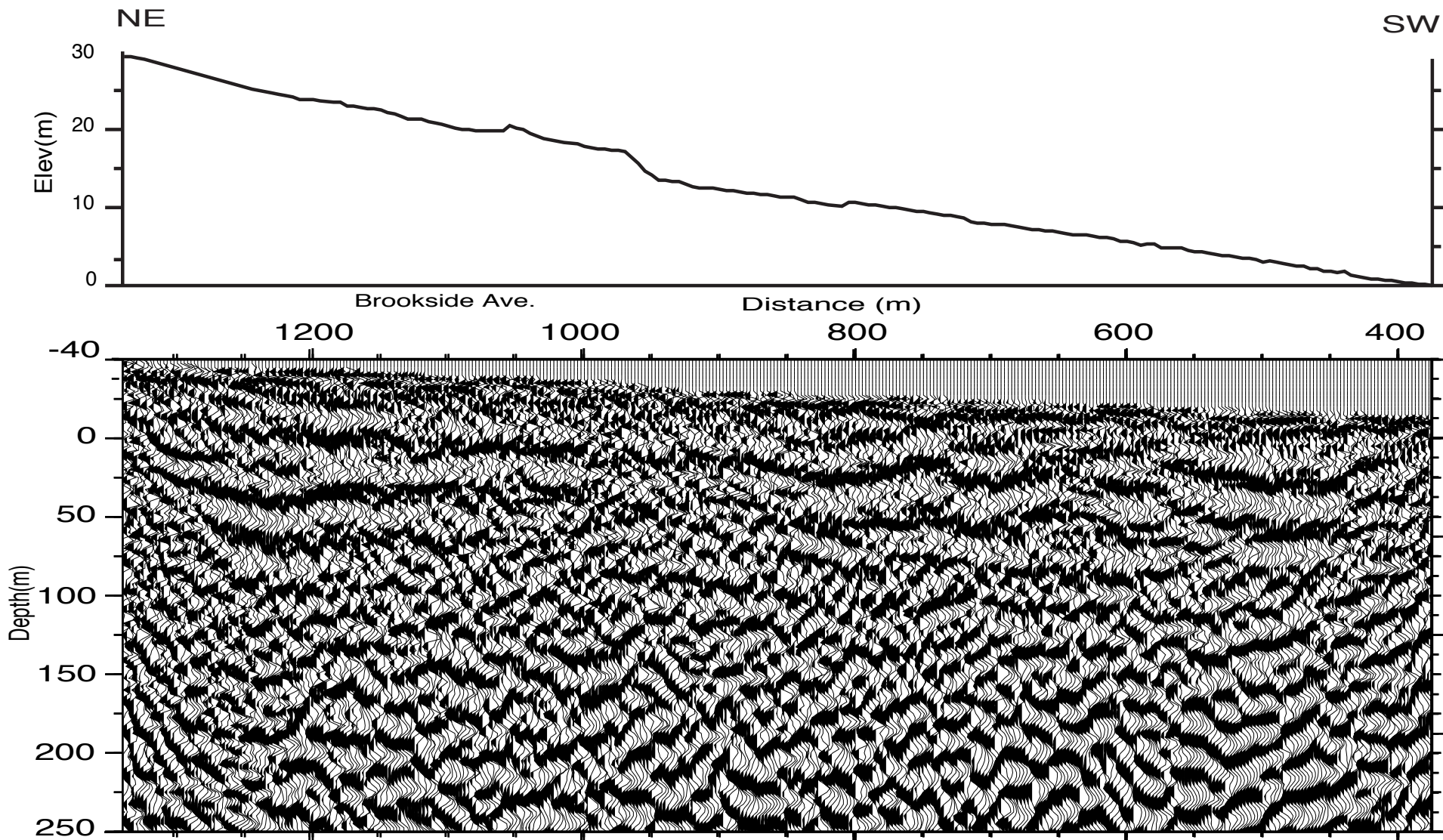


Figure 15

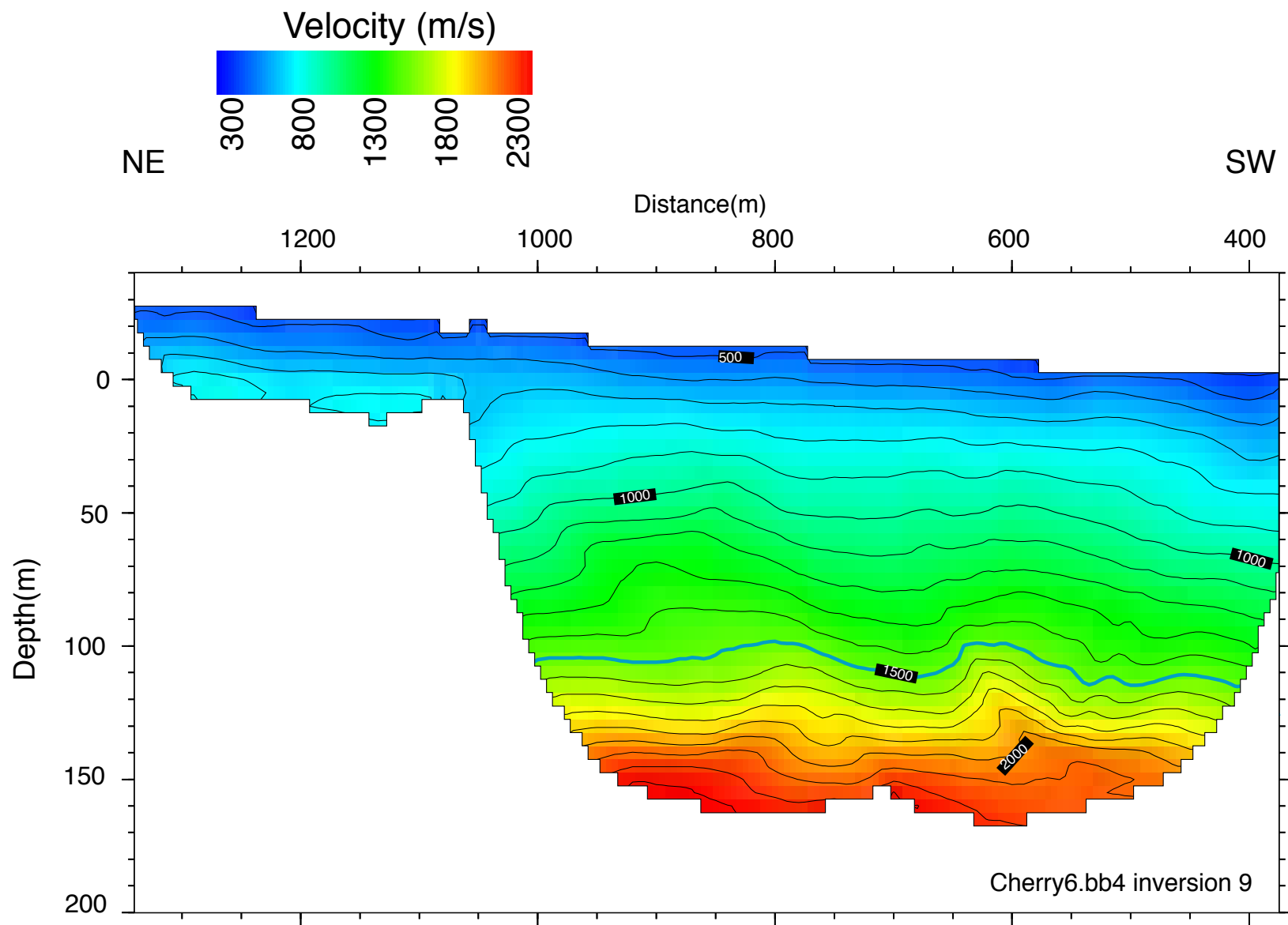


Figure 16

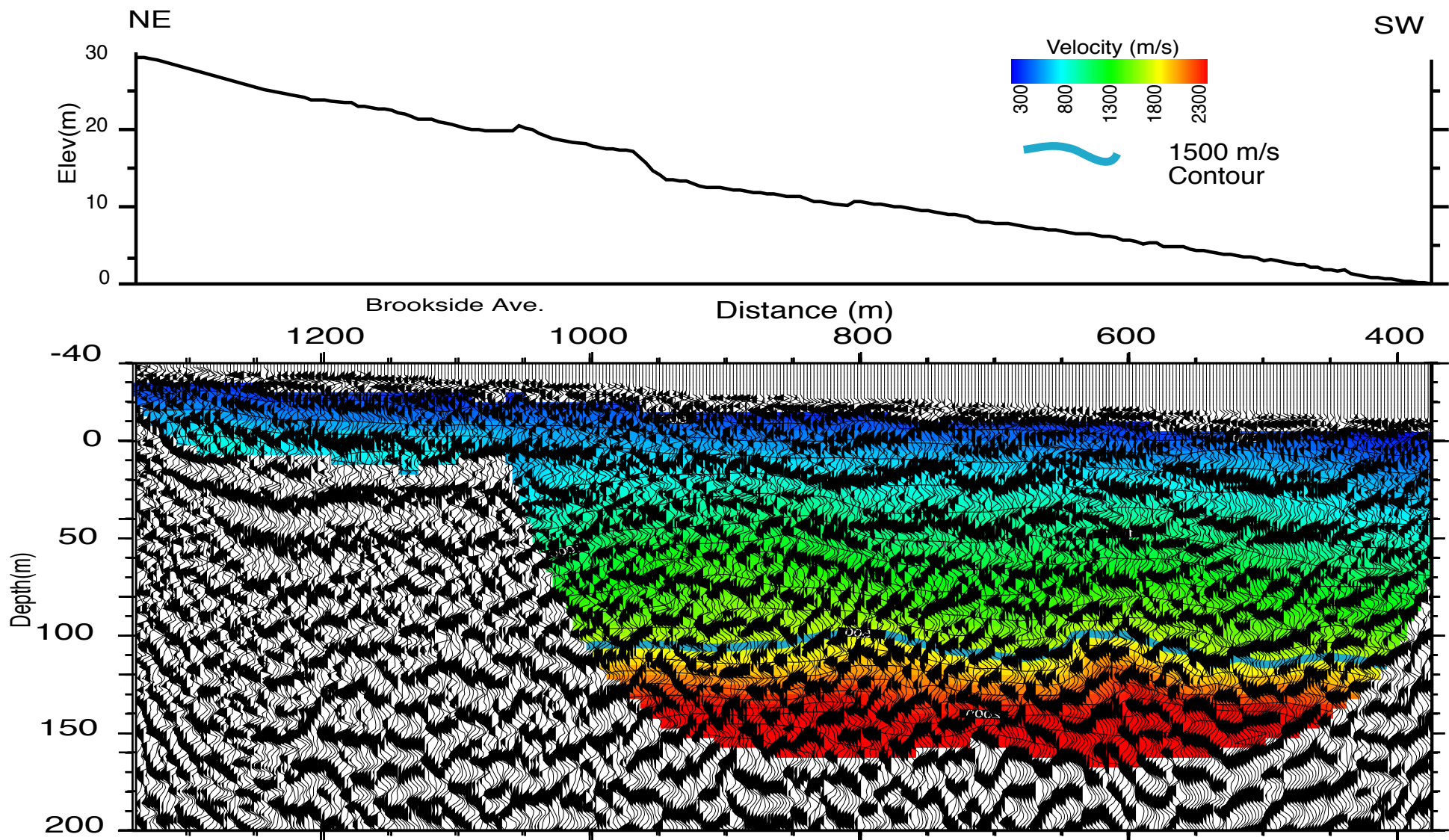


Figure 17

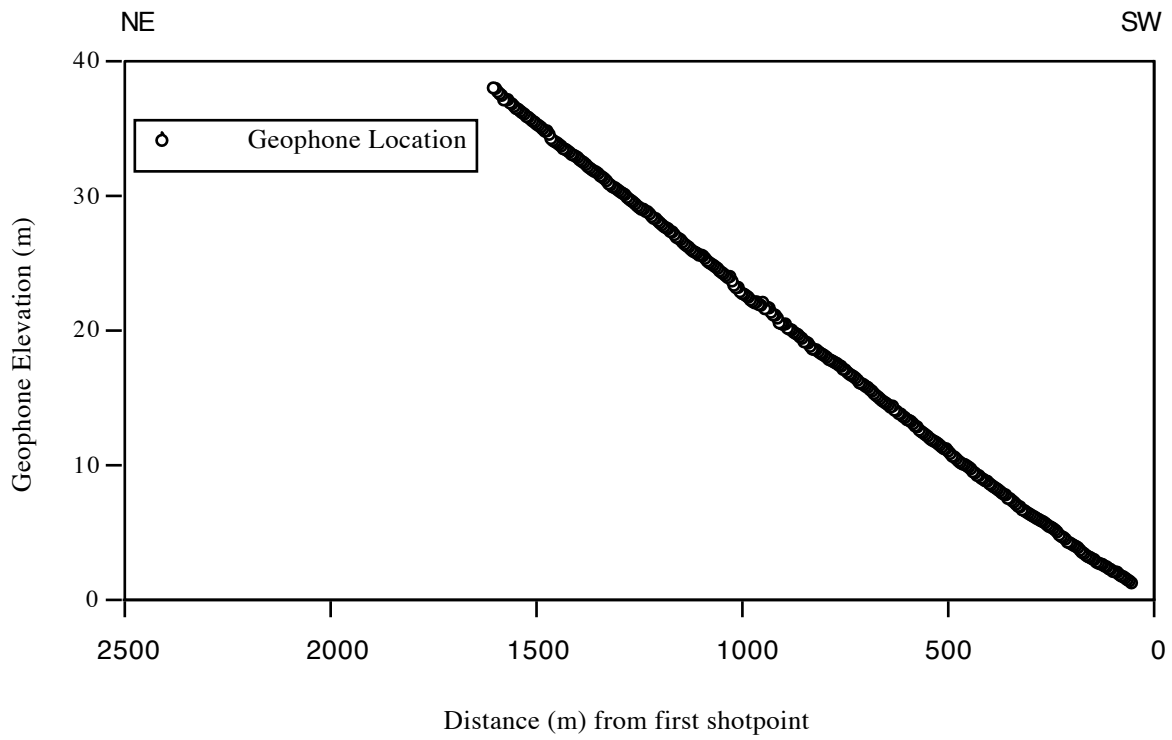


Figure 18

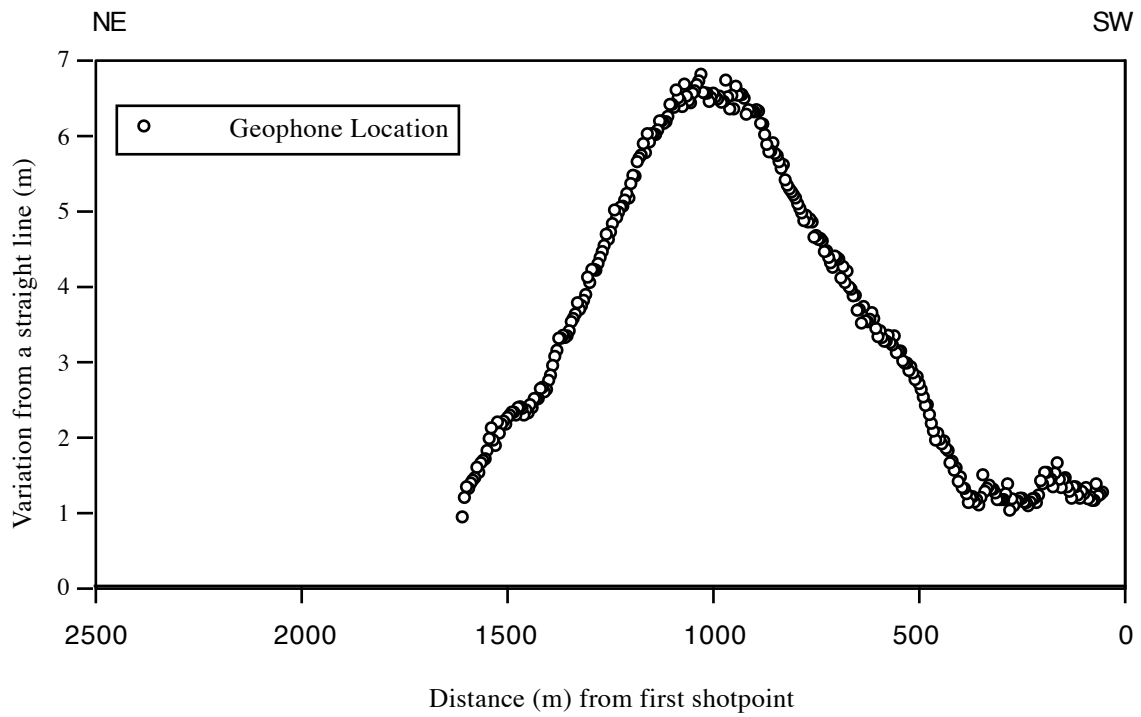


Figure 19



Figure 20



Figure 21

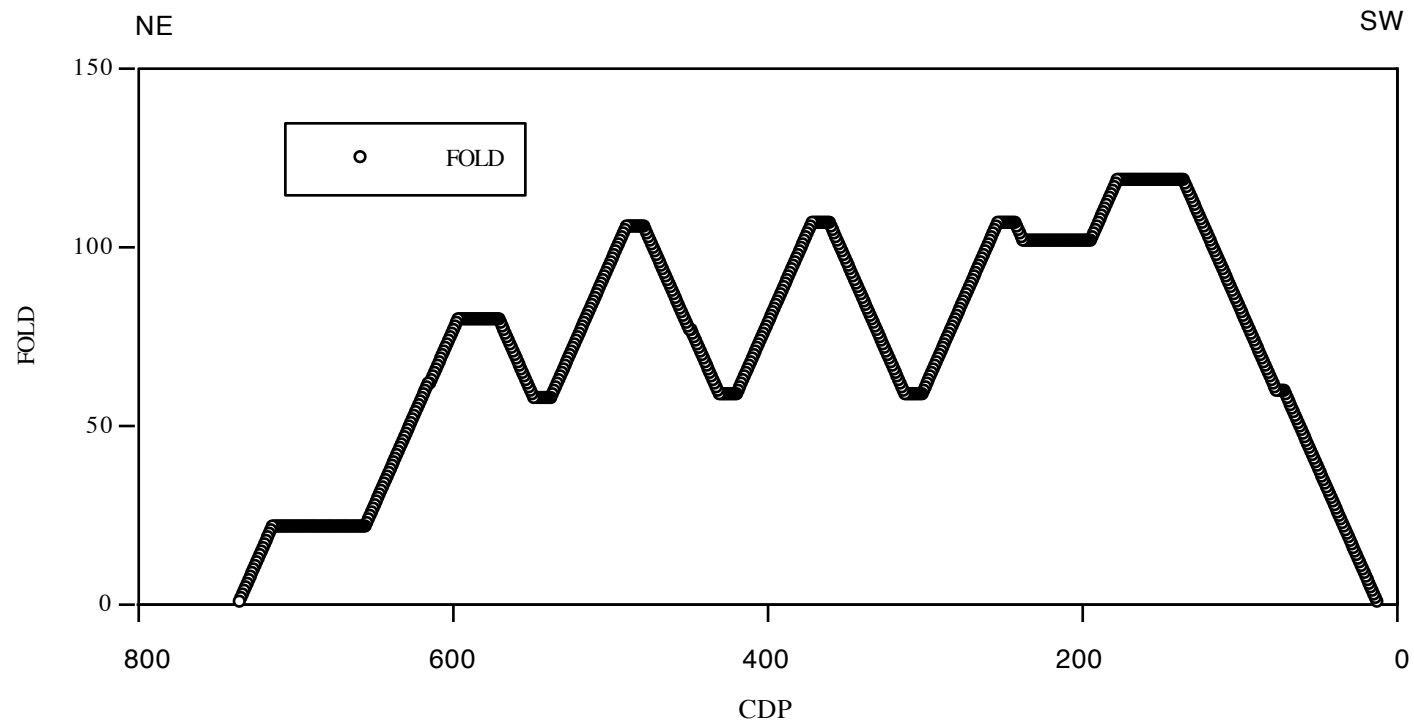


Figure 22

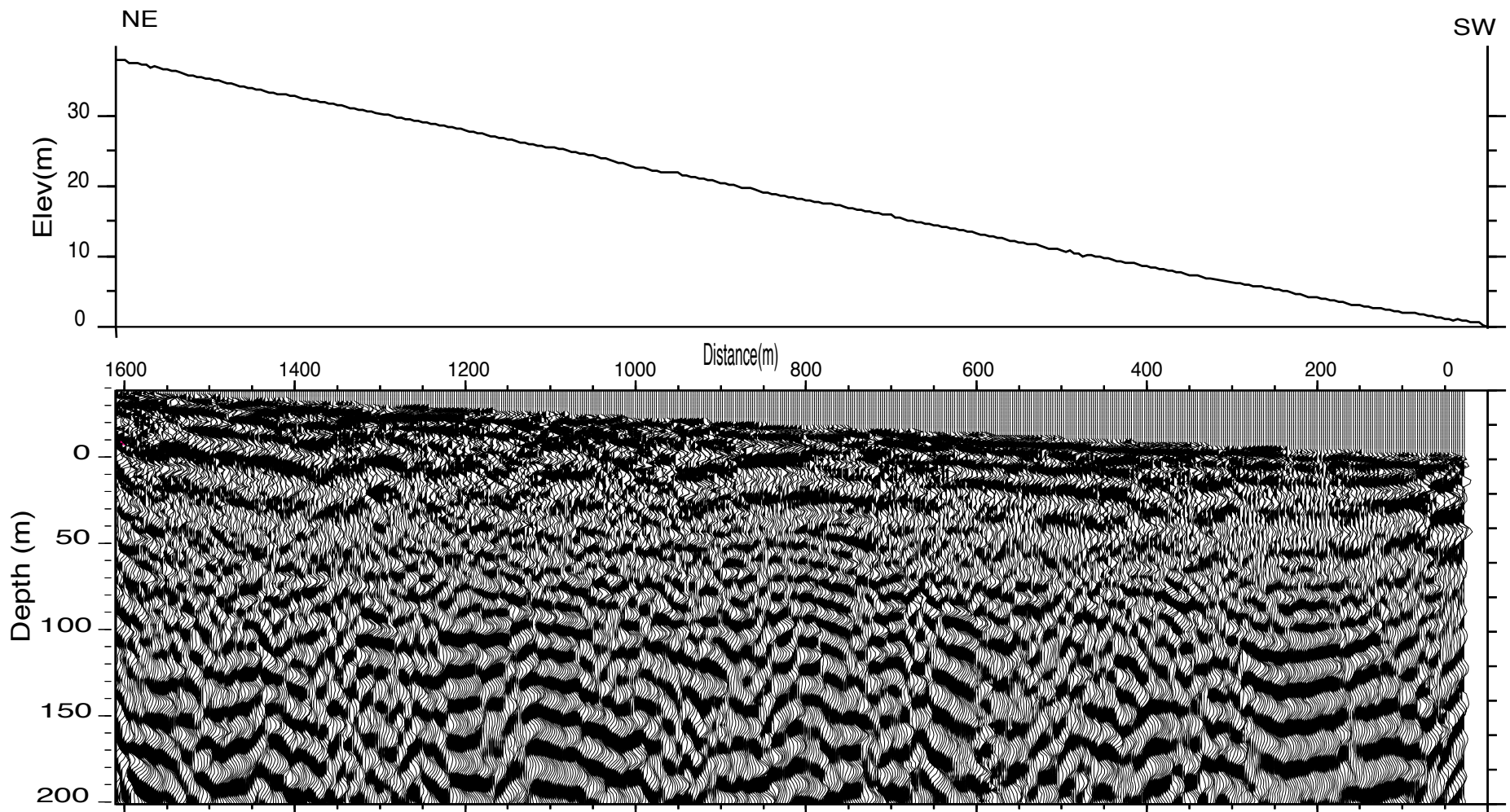


Figure 23

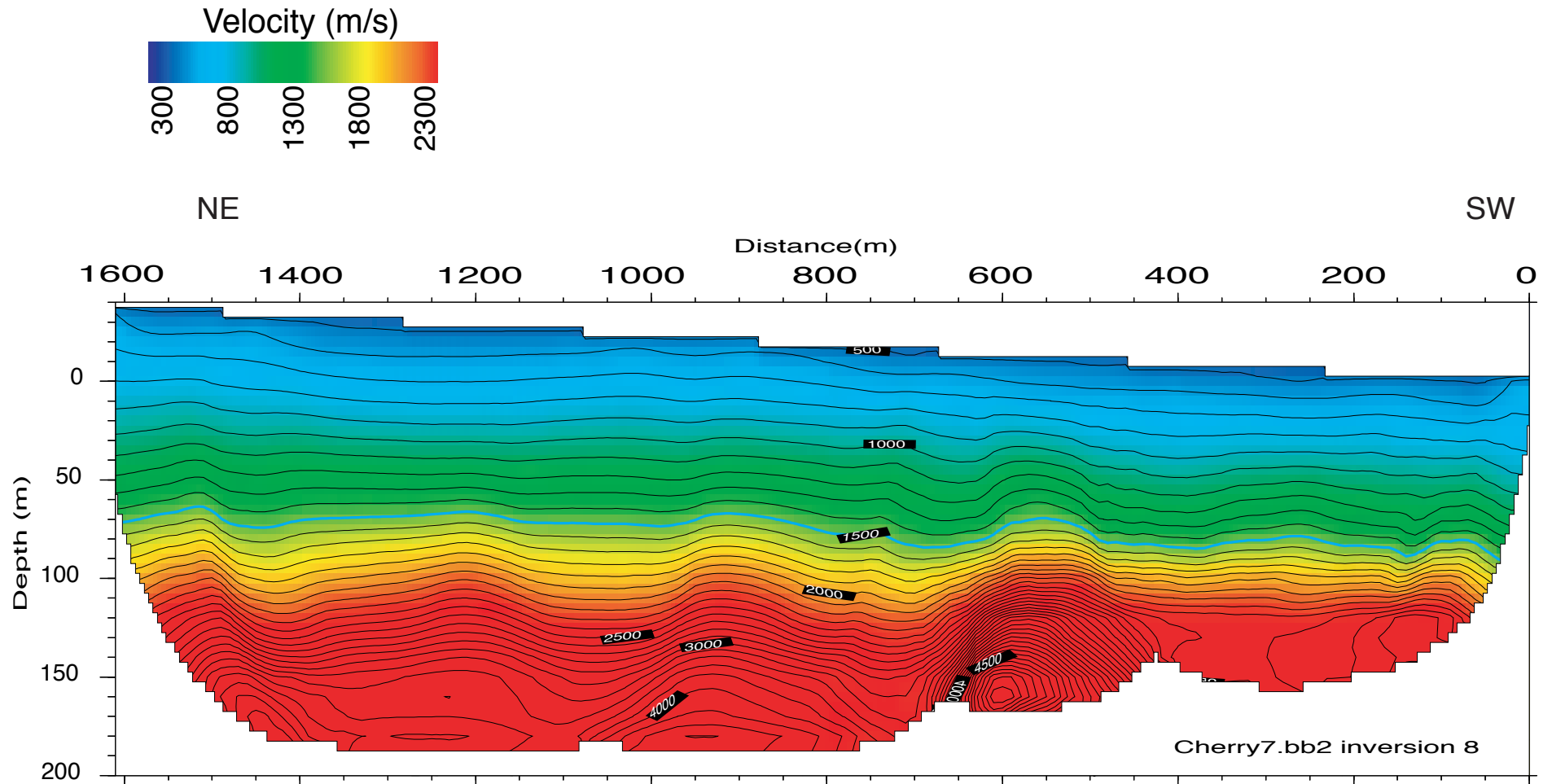


Figure 24

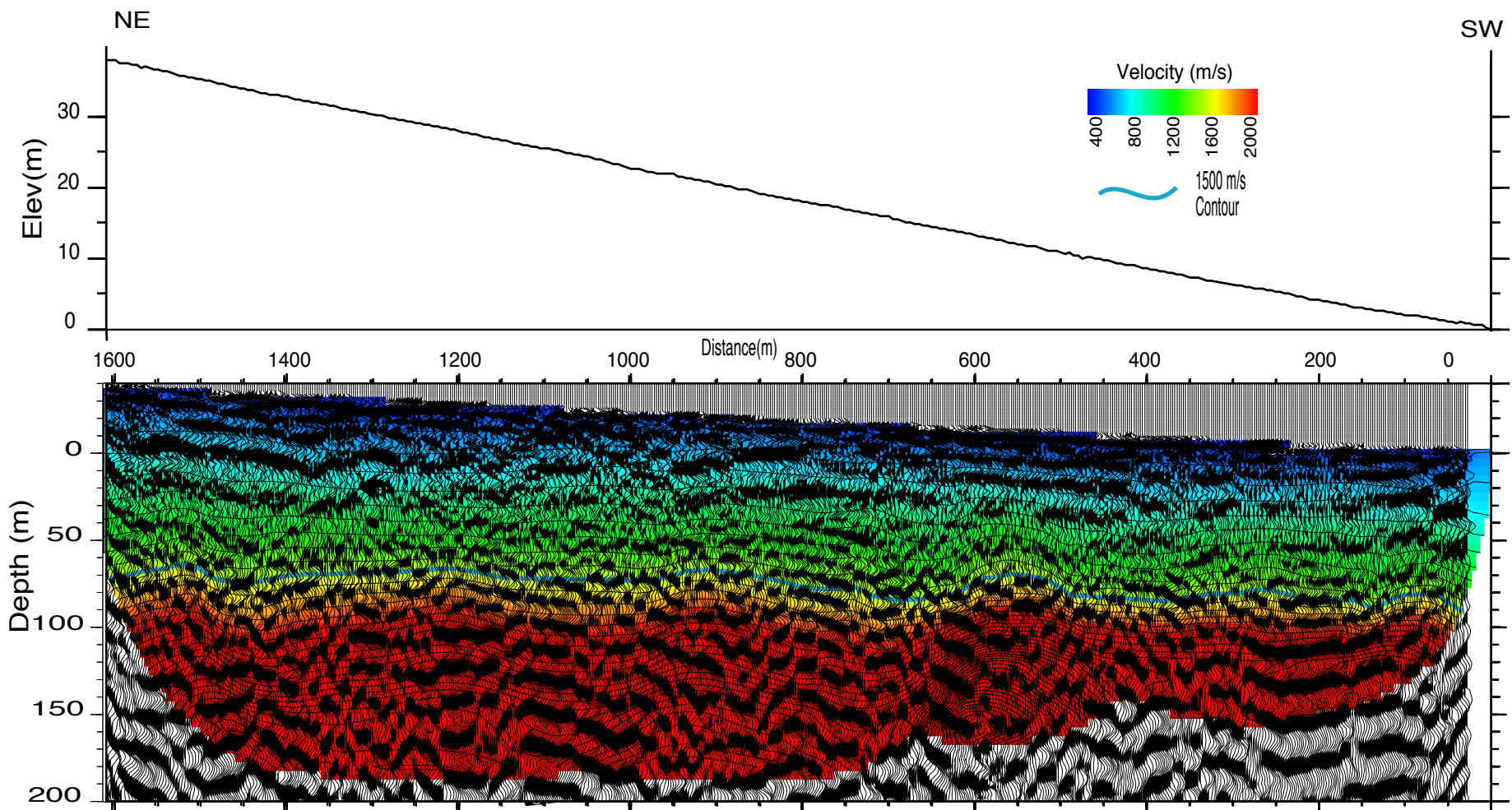


Figure 25

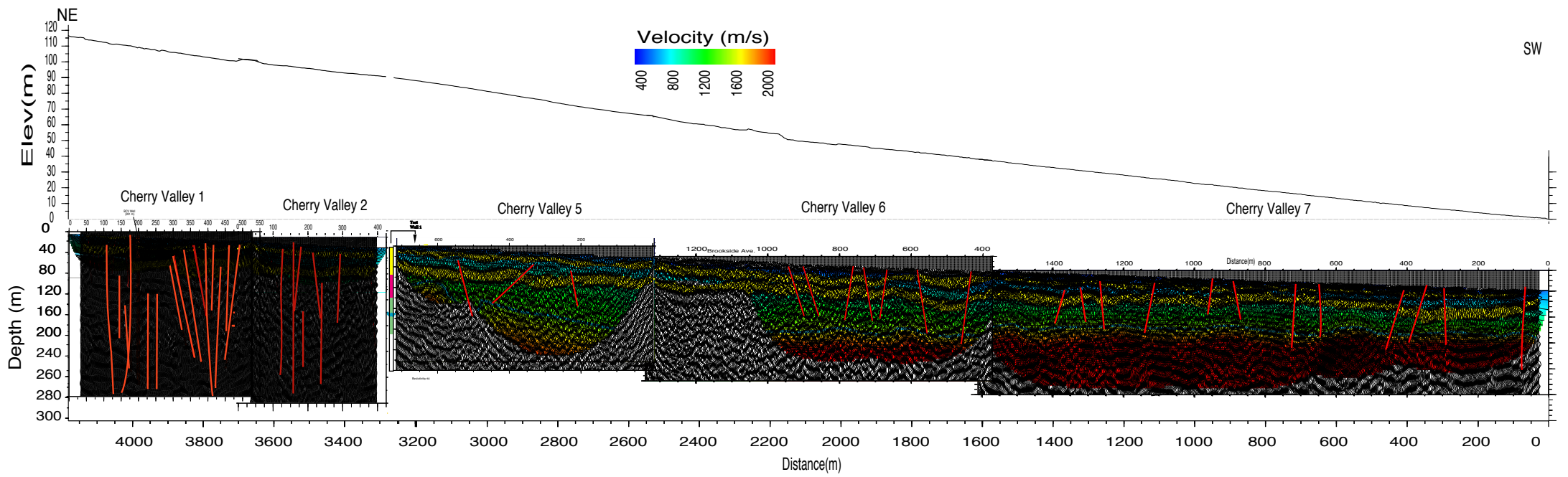


Figure 26a

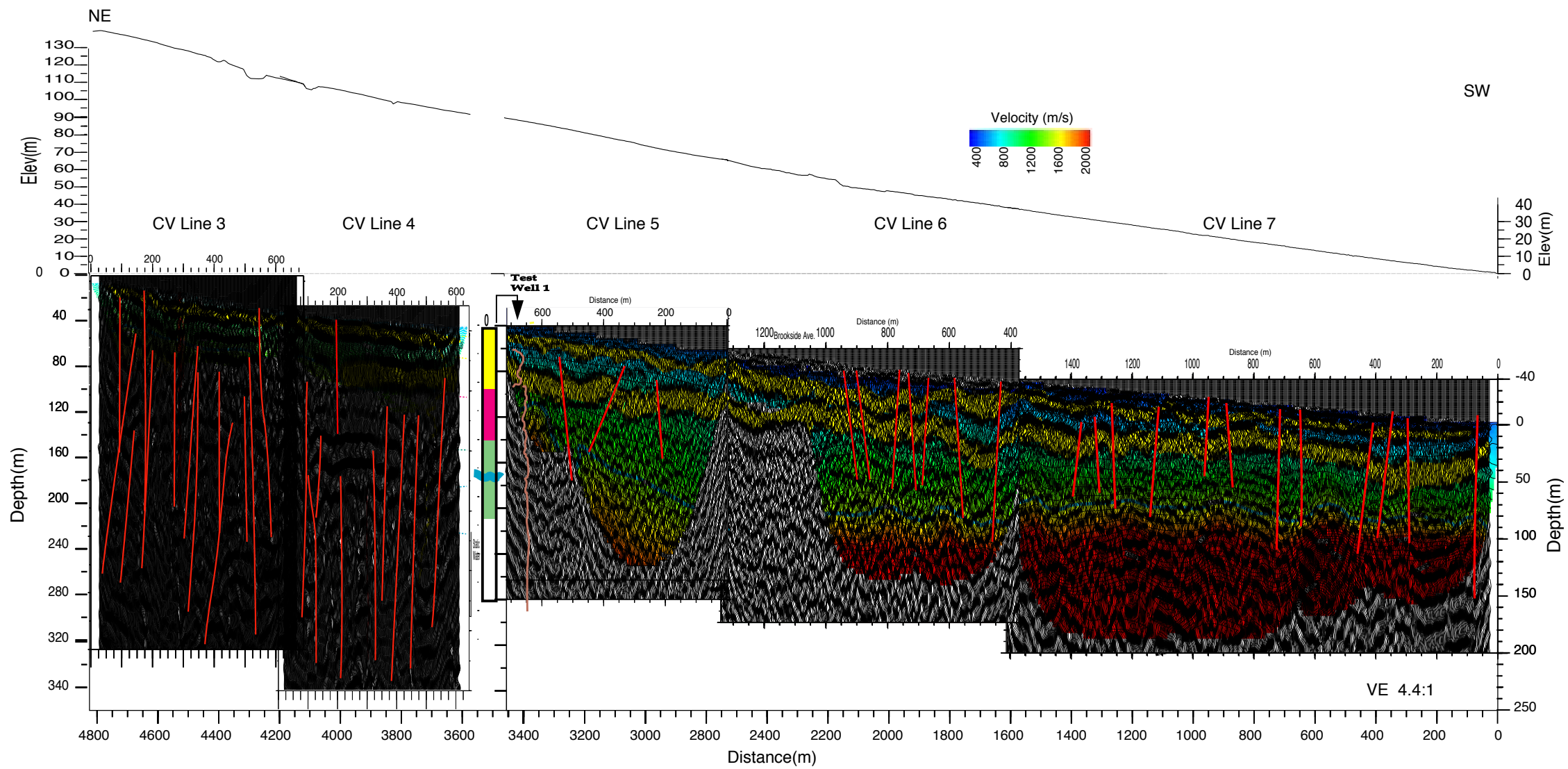


Figure 26b

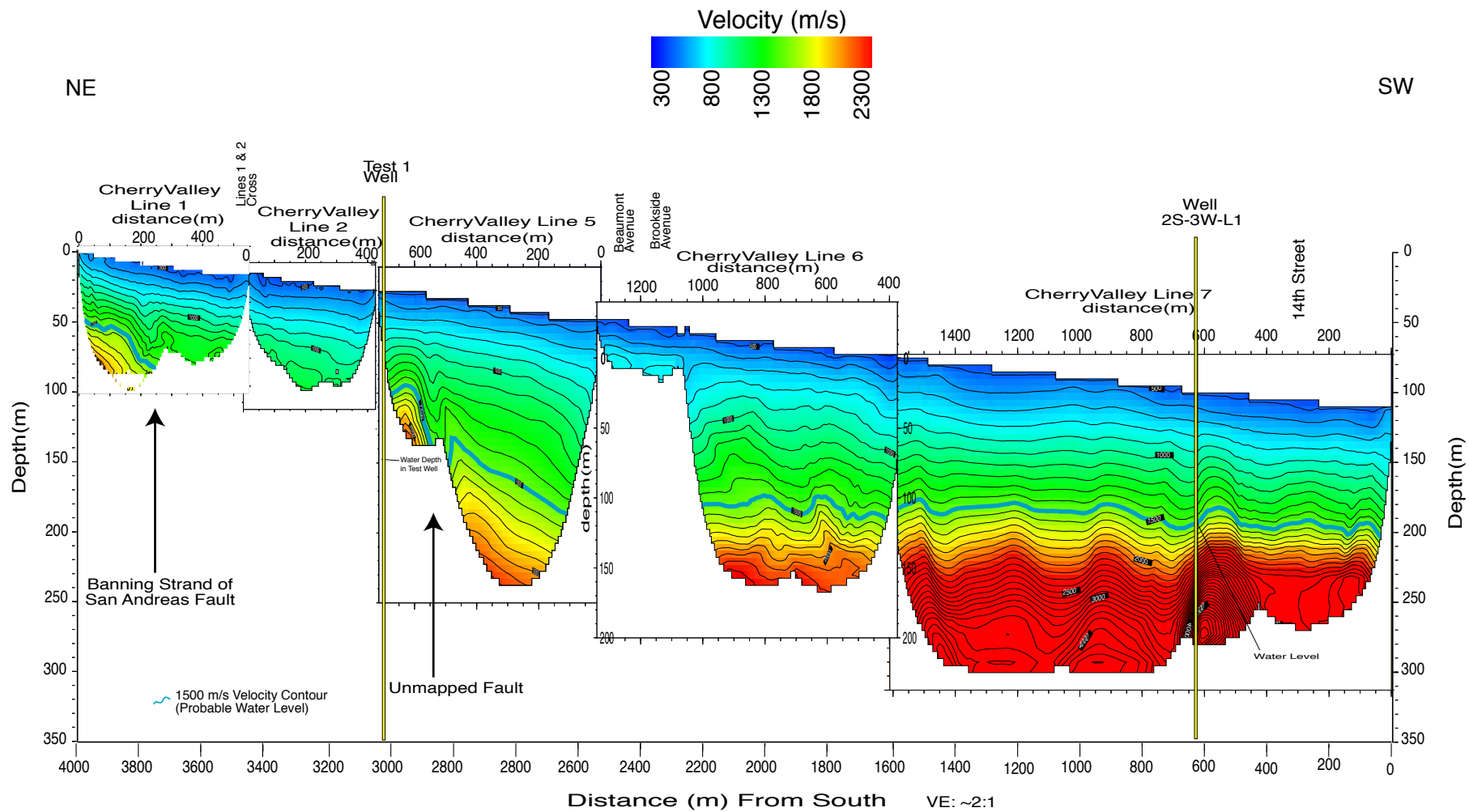


Figure 27a

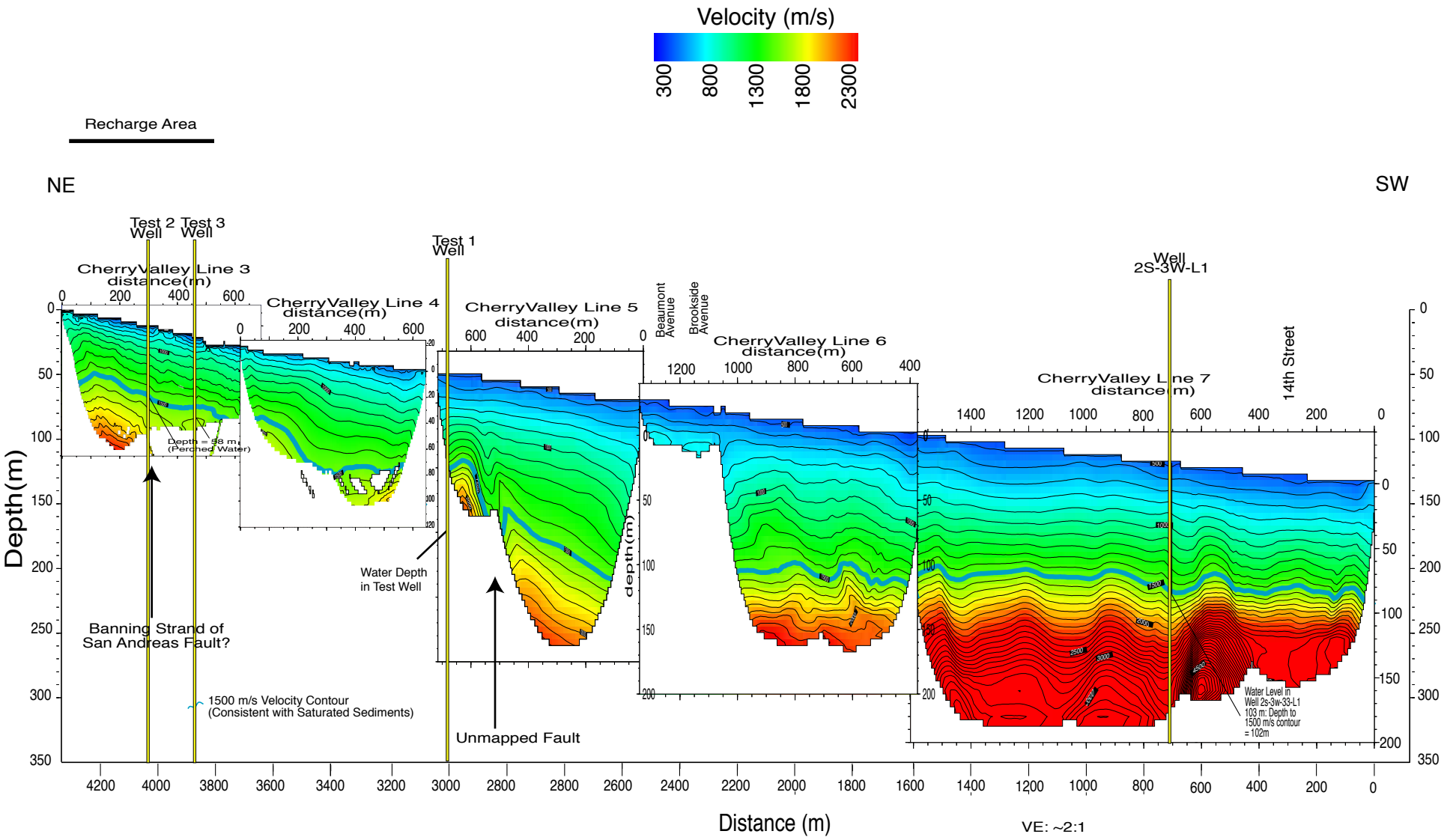


Figure 27b

117°00'

116°57'30"

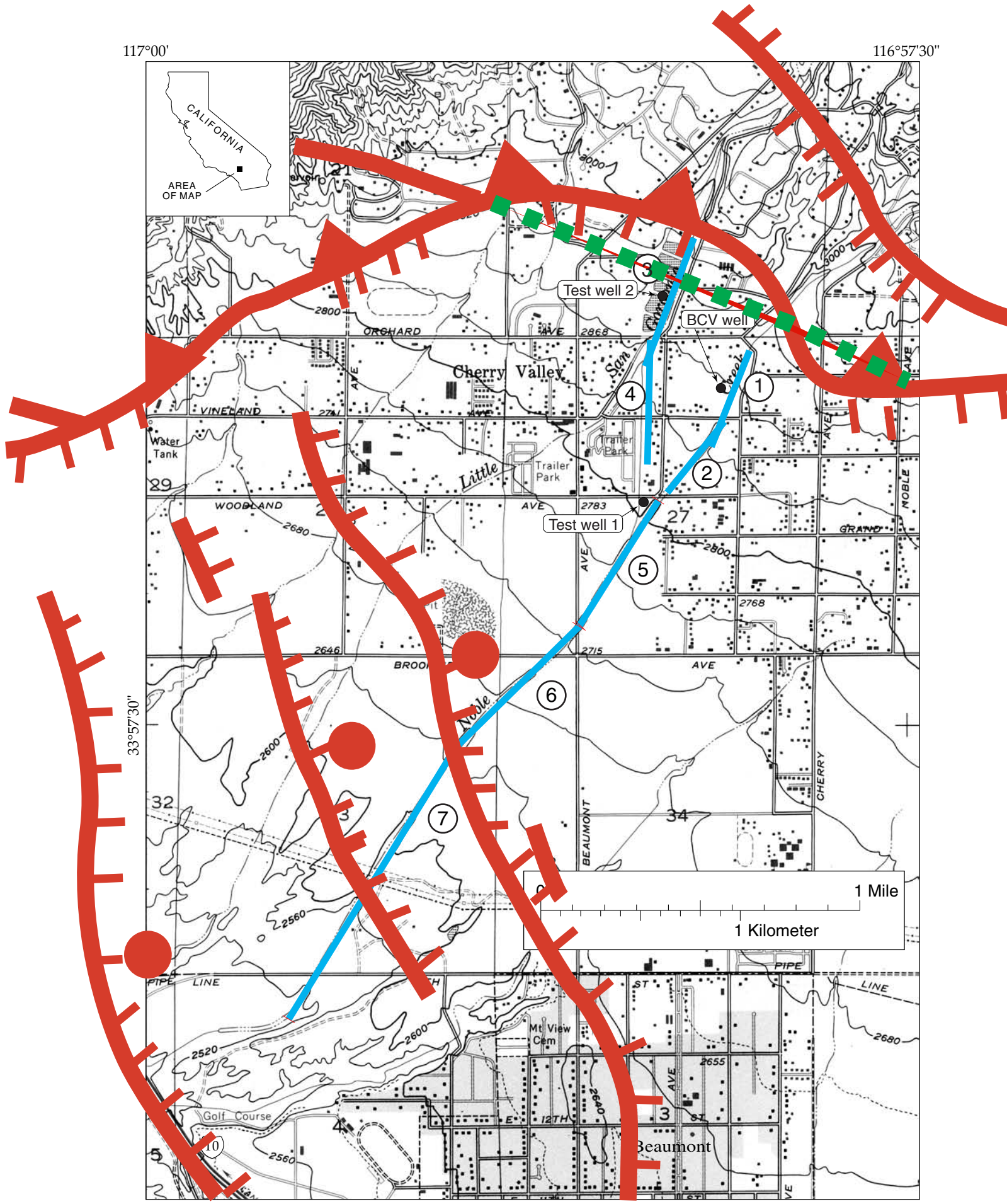


Figure 28